Journal of Volcanology and Geothermal Research 445 (2024) 107972

Contents lists available at ScienceDirect

Journal of Volcanology and Geothermal Research

journal homepage: www.journals.elsevier.com/journal-of-volcanology-and-geothermal-research

Magma storage conditions over the past 4 Ma on Martinique Island, Lesser Antilles

Abigail Martens [a,*], Aurelie Germa [a], Zachary D. Atlas [a], Sylvain Charbonnier [a], Xavier Quidelleur [b]

[a] University of South Florida, 4202 E Fowler, Ave, Tampa, FL 33617, United States of America
[b] Université Paris-Saclay, CNRS, GEOPS, Orsay 91405, France

ARTICLE INFO

Keywords:
Lesser Antilles
Martinique
Thermobarometry
Plagioclase textures
Magma Storage
Volcanic plumbing system

ABSTRACT

We constrain, for the first time, the storage conditions beneath recent (<5 Ma) volcanic edifices in Martinique Island, combining petrography, geochemistry, and thermobarometry. Specifically, we investigate Morne Jacob volcano (5.2–1.5 Ma), Pitons du Carbet complex (998 ka – 322 ka), Trois Îlets Volcanic field (2.35 Ma – 346 ka), and Mt. Conil – Mt. Pelée system (<550 ka). Lava samples range in composition from basalt to dacite, and in age from 4.1 Ma (Morne Jacob) to 1929 CE (Mount Pelée). For the last ~5 Ma, the volcanoes in Martinique were fed by andesitic to dacitic magma stored in the upper 6 km of the crust, at temperatures between 900 and 1100 °C. These shallow reservoirs were frequently replenished and remobilized by basaltic and basaltic-andesite magmas originating from the lower crust with temperatures as high as 1200 °C. Erupted products contain simple to more complex mineral assemblages, and plagioclase phenocrysts exhibit textures and compositional profiles typical of antecrysts, identified as (1) normal, (2) oscillatory, (3) sieved, (4) resorbed core, and (5) resorbed rim. All complexes also show a crystallization gap in the middle crust (10–18 km). Trois Îlets, a distributed volcanic field, is the only complex that shows continuous crystallization through the entire crust, distinct magma batches and storage regions for each individual volcano. More importantly, we see drastic changes in terms of rock composition, storage conditions, and crystal populations in pre - and post – collapse lavas. Large flank collapse (> 5 km^3) can induce decompression as large as 5 MPa in the upper crust and as low as 0.1 MPa down to 10–12 km. Such decompression magnitudes might be sufficient to enhance ascent of basaltic magma from depth, initiate dike intrusions in the mid to upper crust, and remobilize shallow silicic reservoirs. Such events are likely to initiate magma mixing in shallow reservoirs. This noteworthy eruption-triggering mechanism may lead to the incorporation of distinct crystal populations and subsequently contribute to heightened rates of eruption. In summary, the magma storage conditions and plumbing system architecture for the recent volcanoes in Martinique closely resemble those observed in other volcanoes within the Lesser Antilles Island Arc, such as Soufriere Hills Volcano or La Soufriere de Guadeloupe. These newly established correlations offer valuable insights that can aid in the assessment of potential future volcanic eruptions.

1. Introduction

Volcanic plumbing systems consist of pockets of eruptible magma distributed within crystalline mushes that make up plutonic systems (Bachmann and Bergantz, 2008; Cashman et al., 2017; Cooper and Kent, 2014). Those mushes are in complex systems that consist of a network of dikes, plugs, and sills, allowing for transport and storage of magma (Burchardt and Galland, 2016; Galland et al., 2018). Pathways of magma ascent and location of storage regions are controlled in part by the crustal structure, where density contrasts and discontinuities are identified as the main controls on magma focusing and ponding (Putirka and Condit, 2003; Kavanagh et al., 2006; George et al., 2016; Deng et al., 2017; Melekhova et al., 2019; Solaro et al., 2019; Ostorero et al., 2021; Balcone-Boissard et al., 2023). The transfer of deeper magmas into shallower reservoirs allows for mixing and crystal remobilization, and such disequilibrium mineral assemblages are preserved in the erupted record (Bachmann and Bergantz, 2008). Several studies identify magma mixing as an important process controlling the chemical evolution of

* Corresponding author at: School of Geosciences, University of South Florida, 4202 E Fowler avenue, Tampa, FL-33620, United States of America
E-mail address: abigail.e.martens@gmail.com (A. Martens).

https://doi.org/10.1016/j.jvolgeores.2023.107972
Received 26 April 2023; Received in revised form 17 November 2023; Accepted 20 November 2023
Available online 25 November 2023

magmas. For example, intrusion of a basaltic magma into shallow differentiated reservoirs can remobilize crystal mushes and trigger explosive eruptions (Druitt et al., 2002; Halama et al., 2006; Martel, 2012; Rowley, 1978; Samper et al., 2009; Westercamp and Traineau, 1983).

Evidence suggests that structural and morphological changes at the surface, such as flank collapses, also directly affect the chemistry and petrography of erupted magmas and eruptive styles. For instance, unloading associated with a flank collapse may allow for dense primitive magma to reach the surface (Boulesteix et al., 2012; Bachmann and Bergantz, 2008; Boudon et al., 2013; Pinel and Jaupart, 2000). Comparison of pre- and post- collapse lava compositions show that edifice growth promotes eruption of SiO_2 - rich lavas (Borgia et al., 2000; Pinel and Jaupart, 2000), whereas collapse-induced unloading allows the eruption of more mafic magmas that were filtered by the evolved plumbing system prior to the collapse (Pinel and Jaupart, 2000) The collapse of a volcano's flank consistently results in a reduction of pressure within the underlying storage regions (Pinel and Jaupart, 2000). The sudden reduction in mass can impact the buildup of reservoir pressure and conditions for failure in the magma plumbing system, leading to dike intrusions and substantial changes in its chemical evolution (Pinel and Jaupart, 2005; Manconi et al., 2009; Pinel and Albino, 2013). When the shallower reservoirs are interconnected with deeper magma sources, the reduction in pressure is anticipated to trigger a relatively rapid replenishment of the shallow reservoirs by deeper mafic magmas (Acocella, 2021). Understanding the storage conditions of magmas, i.e., temperature, pressure, depth, and water content, and how they change through time and space is key in understanding the eruptive behavior of a volcanic system or region.

The Lesser Antilles arc (Fig. 1) is one of the most studied island arcs in the world for multiple reasons. Its chemical characteristics have been extensively studied, especially considering along-arc and across arc variations (Macdonald et al., 2000; Labanieh et al., 2010, 2012; Cooper et al., 2020; Atlas et al., 2022). Several active volcanoes have erupted in the last two centuries, with the 1902 Mt. Pelée eruption being among the deadliest eruptions recorded in human history. The Lesser Antilles volcanoes display a large variety of eruptive styles (lava flows, domes, Vulcanian to Plinian eruptions, ignimbrites), volumes (<0.1 to >5 km^3 per eruption), and magma compositions (basalt to rhyolite) (Boudon et al., 2017; Macdonald et al., 2000; Pichavant et al., 2002). Many studies reveal that magma mixing is a common process that triggers explosive eruptions at recent (<5 Ma) volcanoes in the Lesser Antilles, especially at Mt. Pelée, Martinique (Annen et al., 2008; Boudon and Balcone-Boissard, 2021; Fichaut et al., 1989), St. Eustatius (Cooper et al., 2019), Soufriere Hills, Montserrat (Druitt et al., 2002), Dominica (Cashman et al., 2017), and Soufrière, Saint Lucia (Bezard et al., 2017). Also, most of the Lesser Antilles islands experienced >15 flank collapses in the past 12 kyr (Boudon et al., 2007). Such catastrophic eruptions are often followed by periods of high eruptive rates and changes in chemistry, indicating a direct effect on the plumbing systems (Boudon et al., 2007). It is therefore important to characterize the conditions and architecture of volcanic plumbing systems beneath the Lesser Antilles to better understand how eruptive styles may change through space and time.

Recent studies provided a detailed view of the crustal structure (Melekhova et al., 2019), volatiles output-input (Cooper et al., 2020; Balcone-Boissard et al., 2023; Bouvier et al., 2008, 2010), and magma storage conditions for several islands (Solaro et al., 2019; Metcalfe et al., 2023; Bezard et al., 2017; Camejo-Harry et al., 2019). Beneath the arc, magmas are being stored in multi-level and transcrustal plumbing systems, with basalts in the lower crust (>25 km), basaltic-andesites in the middle crust (10–18 km), and andesites to rhyolite in the upper crust (<10 km), with focusing of magma at crustal discontinuities especially between the middle and upper crust (Fig. 2a; Balcone-Boissard et al., 2023; Metcalfe et al., 2023; Higgins and Caricchi, 2023). Most studies on the Lesser Antilles focused on the most recent eruptive periods or specific eruptions, and a general lack of knowledge for older systems along the arc remains. For instance, the magma storage conditions in

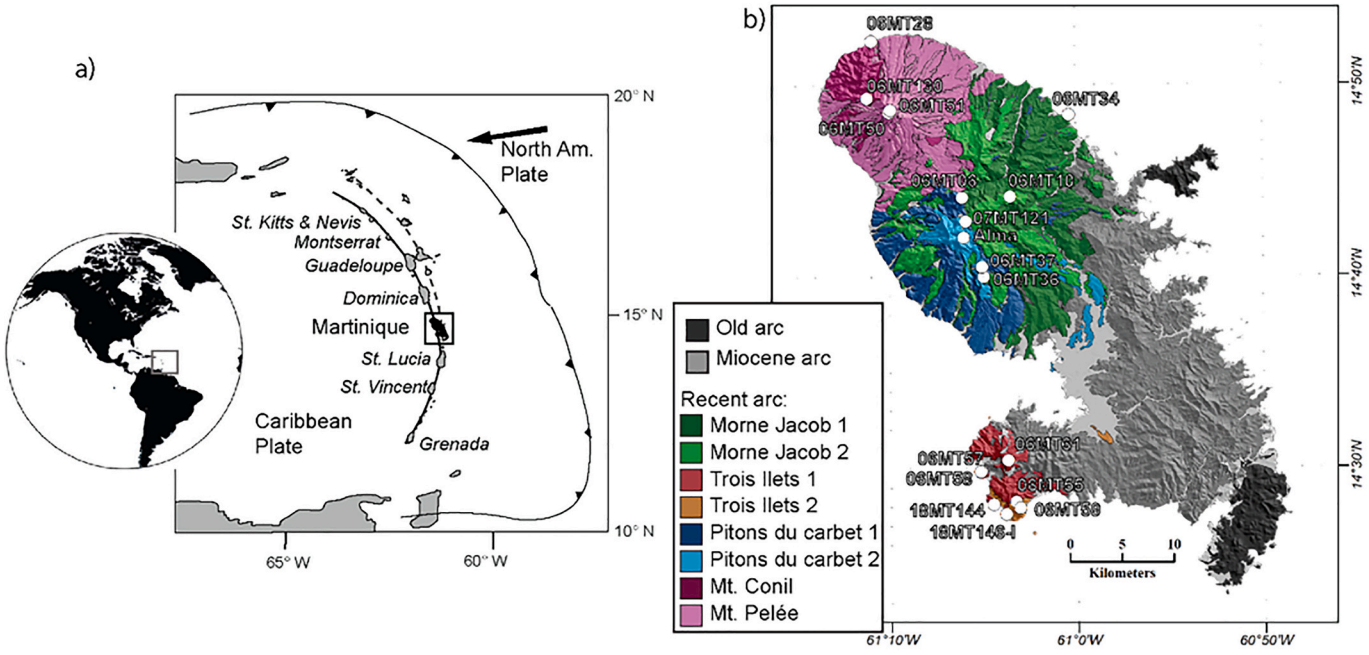

Fig. 1. Location of the study area. (a) Lesser Antilles Island arc setting. Dashed line shows the location of the old arc. Solid black line shows the location of the recent arc. The LAIA is characterized by a single line of islands in the south, and two branches north of Martinique. The eastern branch is the old arc and was active between ca. 40 and 17 Ma (Garmon et al., 2017; Germa et al., 2011a; Legendre et al., 2018; Noury et al., 2021) (b) simplified geological map and digital elevation model of Martinique Island. Old arc (Basal Complex and Sainte Anne Series) and Miocene arc (Vauclin - Pitault Chain and South - western Volcanism) units are represented in gray. Studied edifices are in color: Morne Jacob (green), Pitons du Carbet complex (blue), Trois Îlets volcanic field (red/orange), Mt. Conil and Mt. Pelée (purple and pink). White circles show the location of the 18 samples investigated in this study.

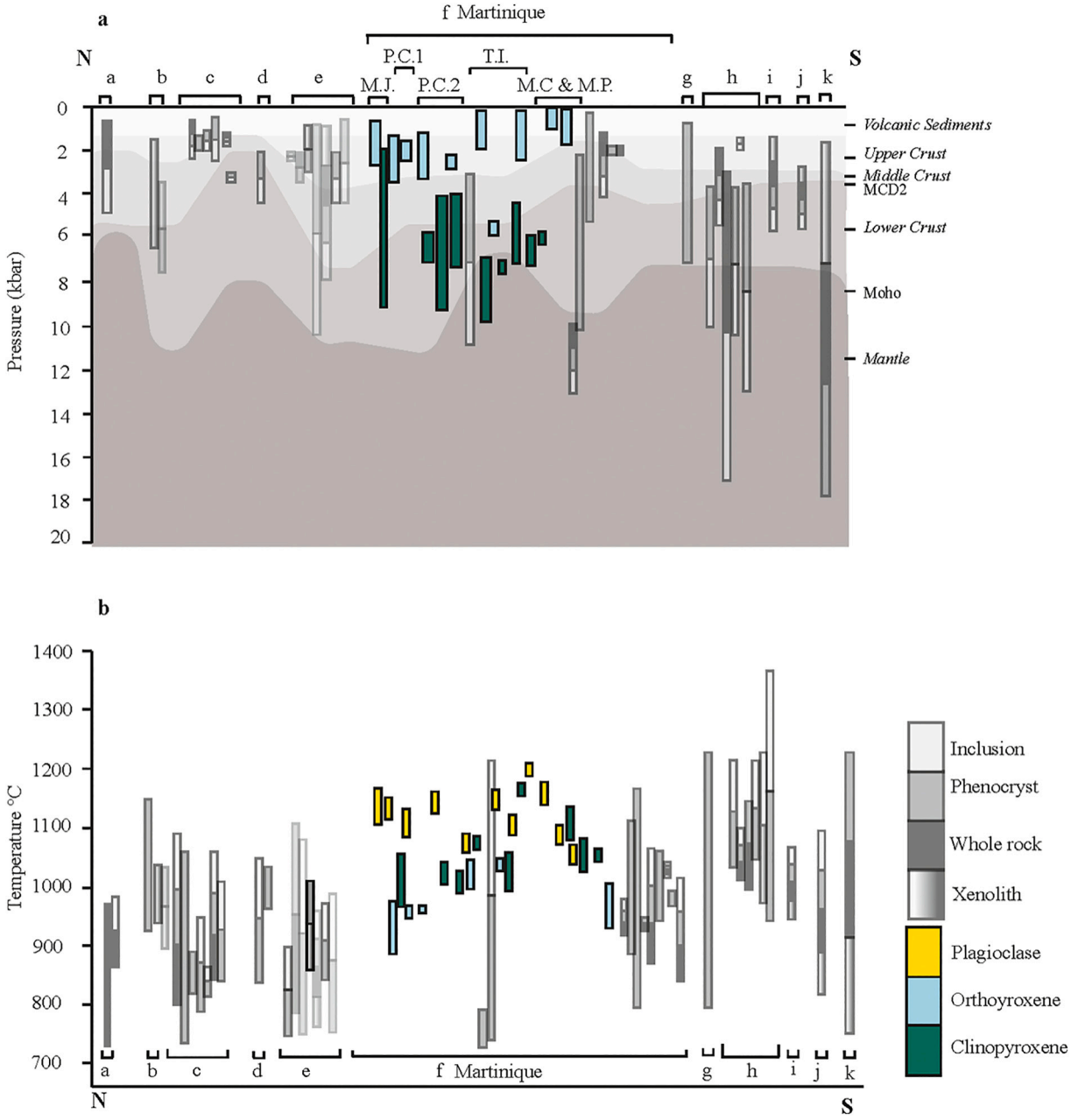

Fig. 2. Crystallization pressures and temperatures throughout the Lesser Antilles. Results from this study are in color and from plagioclase (yellow), orthopyroxene (blue), and clinopyroxene (green). Fig. 2a has Melekhova et al., 2019 crustal layers super imposed onto the pressures ranges throughout the Lesser Antilles. Results from the literature are extracted from melt inclusions (white), phenocrysts (gray), whole rock (black), and xenoliths (gradient). Results displayed from North (left) to South (right) as follows: a: St. Eustatius (Smith and Roobol, 1990; Cooper et al., 2019), (b) St. Kitts (Toothill et al., 2007; Melekhova et al., 2017; Higgins and Caricchi, 2023), (c) Montserrat (Murphy et al., 1998, 2000; Devine et al., 1998; Barclay et al., 1998; Rutherford and Devine, 2003; Zellmer, 2003; Edmonds et al., 2016), (d) Guadeloupe (Pichavant et al., 2018; Metcalfe et al., 2021), (e) Dominica (Gurenko et al., 2005; Lindsay et al., 2005; Halama et al., 2006; Ziberna et al., 2017; Balcone-Boissard et al., 2018; Solaro et al., 2019; d'Augustin et al., 2020); (f) Martinique, (this study, d'Arco et al., 1981; Traineau et al., 1983; Coulon et al., 1984; Fichaut et al., 1989; Gourgaud et al., 1989; Smith and Roobol, 1990; Martel et al., 1998; Macdonald et al., 2000; Pichavant et al., 2002; Annen et al., 2008; Martel et al., 2006), (g) St. Lucia (Bezard et al., 2017), (h) St. Vincent (Bardintzeff, 1984; Bardintzeff, 1992; Heath et al., 1998; Pichavant and Macdonald, 2007; Tollan et al., 2012; Melekhova et al., 2015), (i)Bequia (Camejo-Harry et al., 2018), (j) Kick - 'em - Jenny & Kick - 'em - Jack(Camejo-Harry et al., 2019), (k) Grenada (Stamper et al., 2014). (For interpretation of the references to color in this figure legend, the reader is referred to the web version of this article.)

Martinique are well constrained for Mt. Pelée, specifically the recent (<13,500 yr B.P.) period. Recent eruptions at Mt. Pelée tapped magmas stored at 7–12 km and 840–900 °C in a vertically elongated and zoned reservoir (Fig. 2; Annen et al., 2008; Boudon and Balcone-Boissard, 2021; Gourgaud et al., 1989; Martel et al., 1998; Pichavant et al., 2002). Arriving basaltic magma triggering eruptions at Mt. Pelée have temperatures of about 1050 °C (Bourdier et al., 1985; Martel et al., 1998; Pichavant et al., 2002).

We constrain storage conditions for the older phases of Mt. Pelée and the other recent (<5 Ma) volcanoes along the west coast of Martinique (Fig. 1b), with aims to further constrain the changes in storage conditions in space and time. We constrain storage conditions of Morne Jacob, a basaltic to andesitic shield volcano (5.2–1.5 Ma, Germa et al., 2010), as well as Trois Îlets Volcanic Field, a group of distributed small-volume basaltic to andesitic volcanoes (2.35 Ma – 346 ka, Germa et al., 2011b) not previously investigated for detailed variations in mineral

chemistry. We also focus on Piton du Carbet complex, a cluster of large volume lava domes (998 ka – 322 ka, Germa et al., 2011b), and Mt. Conil – Mt. Pelée system (< 550 ka). Eruptive styles, compositions, mineral assemblages, and volumes are strikingly different for these four complexes (Westercamp et al., 1989; Westercamp and Tazieff, 1980; Fichaut et al., 1989; Labanieh et al., 2012; Labanieh et al., 2010).In this study, we combine geochemical and petrological investigations to constrain the storage conditions beneath each of these volcanic complexes. We specifically constrain (1) plagioclase textures and compositions, (2) plagioclase - liquid equilibrium temperatures, (3) magma water content, and (4) pyroxene - liquid equilibrium temperatures and pressures. We then assess the evolution of these parameters through time and in relation to morphological changes (flank collapse) using published radiometric ages (Germa et al., 2010; Germa et al., 2011b). Constraining the magma storage conditions throughout Martinique will help understand the link between spatial and temporal chemical variations, storage conditions, and diversity of volcanic eruptive styles along the recent Lesser Antilles Island Arc (LAIA).

Our study is timely as, since December 2018, Mt. Pelée is experiencing a new phase of volcanic unrest. Although the probability of short-term eruptive activity is still low at time of writing (August 2023), improving our understanding of Martinique volcanic systems will improve current forecasting models. Indeed, apart from the recent eruptions of Mt. Pelée, little is known about the storage conditions and their evolution through space and time beneath the island. Volcanic systems in Martinique are closer together than any of the active volcanoes of the LAIA, probably because of a higher magma production rate and heat flux in the central portion of the arc than elsewhere (Higgins and Caricchi, 2023). Constraining the storage conditions beneath individual volcanoes in Martinique should help develop a better picture of the volcanic plumbing systems. Our study brings a new spatio-temporal perspective on the evolution of magma storage systems beneath the recent Lesser Antilles arc. Understanding how magma storage and ascent are influenced by morphological changes at the surface will provide clues to the possible evolution of volcanic systems.

2. Geological setting

2.1. Lesser Antilles Island arc

The Lesser Antilles island arc (LAIA, Fig. 1a) is related to the subduction of the North American plate under the Caribbean plate and has been active for >40 Ma (Allen et al., 2019; Bouysse et al., 1990; Germa et al., 2011a; Macdonald et al., 2000).

The volcanic products on the islands of the north-eastern branch are now covered by carbonate platforms. In the south, rocks from the old arc outcrop in Grenada and the Grenadines as calc - alkaline dikes, volcanic rocks, and volcaniclastic deposits. The central islands show well - developed volcanic units in eastern St Lucia, Martinique, and Dominica (Bouysse et al., 1985; Briden et al., 1979; Germa et al., 2011a; Rojas-Agramonte et al., 2017). During the Miocene and Pliocene (18 to 7 Ma), volcanism continued only in Martinique (Westercamp and Tazieff, 1980; Germa et al., 2011a). Volcanic activity along the recent arc started <6 Ma (Germa et al., 2011a; Macdonald et al., 2000) and built the islands of Saba, St. Eustatius, St. Kitts, Nevis, Montserrat, Basse - Terre (west Guadeloupe), Dominica, western coast of Martinique, St. Lucia, St. Vincent, the Grenadines, and Grenada.

2.2. Lesser Antilles crustal model and magma storage conditions

Moho depth beneath the Lesser Antilles varies between 25 and 37 km (Melekhova et al., 2019; Schlaphorst et al., 2018; Balcone-Boissard et al., 2023). The crust is made of four layers, corresponding to the lower crust, middle crust, upper crust, and volcaniclastics and sediments in the upper 5 km (Kopp et al., 2011; Melekhova et al., 2019). The compositions and thicknesses of each layer are different beneath each island (Fig. 2a; Melekhova et al., 2019).

Volcanoes of the recent arc share similar magma storage conditions and architecture, with vertically extensive multi-layer magmatic systems whose location is controlled by the structure, thickness, and composition of the crust (Solaro et al., 2019; Metcalfe et al., 2023; Balcone-Boissard et al., 2023; Higgins and Caricchi, 2023). Mantle-derived basaltic magmas are injected in the lower crust and later evolve by fractional crystallization, mixing, and assimilation (Annen et al., 2008; Bezard et al., 2017; Boudon and Balcone-Boissard, 2021; Camejo-Harry et al., 2019; Zellmer, 2003). Most islands have magma storage zones near the boundary between the upper and middle crust, as well as deeper storage zones near the middle-lower crust boundary (Fig. 2a; Balcone-Boissard et al., 2023). For instance, basaltic - andesites are stored around 15–30 km beneath Martinique and St. Vincent (Heath et al., 1998; Pichavant et al., 2002; Martel et al., 2006), but are found in shallower regions (8–12 km) beneath St Lucia and Kick - em' - Jenny (Bezard et al., 2017; Camejo-Harry et al., 2019). Most of the andesitic to dacitic storage concentrates in the upper crust around a depth of 3 to 8 km depth (Annen et al., 2008; Camejo-Harry et al., 2019; Camejo-Harry et al., 2018; Cooper et al., 2019; d'Augustin et al., 2020; Melekhova et al., 2019; Pichavant et al., 2018; Stamper et al., 2014; Tollan et al., 2012; Higgins and Caricchi, 2023). However, it appears that explosive or large ignimbrite eruptions, as in Dominica for instance, may sample only mid-crustal reservoirs (Solaro et al., 2019). Typical storage temperatures of Lesser Antilles magma vary from 1130 to 1180 °C for basalts, 1050–1060 °C for basaltic andesite, and 740–960 °C for andesite - dacites (Fig. 2b).

The recent volcanoes along the LAIA show that eruptions are frequently triggered following the injection of a mafic magma (>1025 °C) into a differentiated and relatively cold felsic reservoir (~825 °C) (Barclay et al., 1998; Devine et al., 1998; Edmonds et al., 2016; Murphy et al., 2000; Zellmer, 2003. Halama et al., 2006; Pichavant et al., 2018; Camejo-Harry et al., 2019) (Fig. 2). For instance, magmas that erupt at Soufriere Hills volcano (Montserrat) were stored in reservoirs located between 5 and 16 km with an average temperature of 860 °C periodically replenished by mafic magma (Barclay et al., 1998; Devine et al., 1998; Edmonds et al., 2016; Murphy et al., 2000; Zellmer, 2003) (Fig. 2). Evolved magmas erupted from La Soufriere, Guadeloupe, are stored at 6–9 km and 825 °C and can be remobilized by intrusions of moderately hot (975–1025 °C) basaltic magmas (Pichavant et al., 2018; Metcalfe et al., 2022, 2023).

2.3. Martinique island

Martinique is in the center of the LAIA (Fig. 1a). The island consists of eight successive volcanic complexes that migrated from east to west over the last 25 Ma (Bouysse and Guennoc, 1983; Germa et al., 2011a, 2011b; Nagle et al., 1976; Westercamp and Tazieff, 1980). We here focus on the volcanoes that belong to the recent arc and whose eruptive histories have been well described elsewhere (Westercamp and Tazieff, 1980; Andreieff et al., 1988; Germa et al., 2011a, 2011b, 2010) and summarized below. Specifically, and by chronological order, these volcanoes are (1) Morne Jacob (5.2–1.5 Ma, Germa et al., 2010), (2) Trois ÎletsVolcanic Field (2.35 Ma – 346 ka, Germa et al., 2011b), (3) Piton du Carbet complex (998 ka – 322 ka, Germa et al., 2011b), and (4) Mt. Conil – Mt. Pelée system (< 550 ka, Germa et al., 2011b). The recent volcanoes on Martinique are relatively close to each other compared to the average distance between active volcanoes in the LAIA. For instance, Mt. Pelée is 12 km north of the center of Pitons du Carbet complex, which is itself built just over the western flank of Morne Jacob and are both 20 km north of Trois Îlets volcanic field (Fig. 1). In comparison, the average spacing between active volcanoes in the Lesser Antilles is 25–100 km (Wadge, 1986). The relative proximity of the volcanoes in Martinique could be related to a local increase of heat and fluid flux in the central part of the LAIA, (Germa, 2009; Atlas et al., 2022; Higgins and Caricchi, 2023).

Morne Jacob volcano (Fig. 1b) is composed of tholeiitic to calc - alkaline basalts and andesites that erupted from 5.2 to 4.0 Ma and from 3.2 to 1.5 Ma (Germa et al., 2010). The Pitons du Carbet complex sits above the western flank of Morne Jacob volcano (Fig. 1b) and was built between 1 Ma and 325 ka in two main phases separated by a 30–40 km^3 flank collapse (Boudon et al., 2007) about 337 ka ago (Samper et al., 2008; Germa et al., 2010). During the last eruptive phase of Morne Jacob and the activity of Pitons du Carbet complex, another complex was active in the south-western part of the island, named Trois Îlets volcanic field (Fig. 1b), that consists of distributed small volume volcanoes that erupted after a large ignimbrite eruption about 3 Ma (Westercamp et al., 1989). The early activity (3 Ma – 1.5 Ma) consisted of the extrusion of several lava domes and an olivine-bearing basaltic-andesite lava flow (Germa et al., 2011b). Then, five distinct volcanoes erupted along a NW - SE linear volcanic system between ~650 and 350 ka. Each edifice in the Trois Îlets volcanic field displays its own geochemical signature, showing evidence of distinct plumbing systems and remobilization of phenocrysts by complex magmatic processes (Coulon et al., 1984; Germa et al., 2011b). Finally, the most recent volcanic system of Martinique consists of Mt. Conil (~550–127 ka) and Mt. Pelée (<127 ka) in the northern part of the island (Fig. 1b). Mt. Conil was constructed until 127 ka, when its western flank collapsed into the Caribbean Sea (Boudon and Balcone-Boissard, 2021; Germa et al., 2011b; Le Friant et al., 2003a; Roobol and Smith, 1976). A new cone was rapidly constructed into the horseshoe shaped depression as magma production rates increased drastically just after the collapse (Boudon and Balcone - Boissard, 2021). This cone was partially destroyed by a second collapse about 36 ka ago and rapidly followed by renewal of activity and growth of the current cone (Boudon and Balcone-Boissard, 2021; Germa et al., 2011b; Roobol and Smith, 1976, Michaud - Michaud-Dubuy, 2019; Traineau et al., 1983). Magmas erupted just after the second collapse, and for about 10 kyrs after, were more mafic (basaltic andesites) than the ones produced before (Boudon and Balcone-Boissard, 2021). Volcanic activity at Mt. Pelée over the past 5000 years is characterized by sub-Plinian/Plinian and dome-forming eruptions (Westercamp and Traineau, 1983; Boudon et al., 2005). Historical events at Mt. Pelée volcano include two minor phreatic eruptions in 1792 CE and 1851 CE, and two magmatic eruptions in 1902–1905 CE and 1929–1932 CE (Boudon et al., 2005). Starting in December 2018, Mt. Pelée has entered a phase of unrest. The indications of the ongoing unrest have been extensively described (Fontaine et al., 2021, 2022; and https://www.ipgp.fr/observation/ovs/ovsm/rapports-annuels-dactivite-de-lovsm-ipgp/). A better understanding of magma storage conditions over time in Martinique is therefore timely and warranted.

Multiple studies on the most recent eruptions constrained pre-eruptive conditions with H_2O content of 5.3 to 6.3 wt%, and magmas stored at 7–12 km (2–4 kbar) and 840 °C - 900 °C in a vertically elongated and zoned reservoir (Annen et al., 2008; Boudon and Balcone-Boissard, 2021; Bourdier et al., 1985; Fichaut et al., 1989; Gourgaud et al., 1989; Martel et al., 1998; Pichavant et al., 2002) (Fig. 2). Basaltic magma intruding this reservoir and triggering eruptions at Mt. Pelée have temperatures of about 1050 °C (Bourdier et al., 1985; Martel et al., 1998; Pichavant et al., 2002).

3. Methodology

We investigated a total of 17 samples from Martinique Island to characterize plagioclase textures, as well as plagioclase and pyroxene compositions used for thermobarometry calculations. Sixteen of these samples were previously dated (Germa et al., 2010; Germa et al., 2011a, 2011b) and their whole-rock major and trace elements as well as isotopic compositions were determined (Labanieh et al., 2012, 2010). An additional sample was collected in 2018 (18MT146) but has not been dated. We here determine its whole - rock major element compositions to complement our dataset. Sample locations can be found in Table 1 and Fig. 1b, and in Germa et al. (2010; Germa et al., 2011a, 2011b).

Table 1
Sample locations, rock types, and ages.

All samples except 18MT146, 06MT51, and 06MT50 were dated by Germa et al., 2010; Germa et al., 2011a, 2011b

Sample	Latitude	Longitude	Complex	Location Name	Rock Type	Age in ka	Crystallinity	Mineral mode
06MT34	14.8065	−61.0075	Morne Jacob	Pain de Sucre	Basalt	4101 ± 60	5–15%	Pl > CPx - Ox
06MT10	14.7361	−61.0591	Morne Jacob	Morne Bellevue	Orthopyroxene and clinopyroxene bearing andesite	2111 ± 30	20–40%	PL > CPx-Opx-Ox
06MT36	14.6676	−61.0831	Piton du Carbet	Morne Césaire	Hornblende and quartz bearing dacite	998 ± 14	30–45%	Pl > Opx > Qz > Hbde
06MT06	14.7350	−61.1020	Piton du Carbet	Piton Gelé	Hornblende and quartz bearing dacite	770 ± 11	30–45%	Pl > Opx > Qz > Hbde
ALMA	14.7003	−61.1029	Piton du Carbet	Alma	Quartz and biotite bearing dacite	338 ± 5	30–45%	Pl > Opx-CPx > Qz > Hbde-Bt
07MT121	14.7155	−61.0994	Piton du Carbet	Piton Boucher	Quartz and biotite bearing andesite	331 ± 6	30–45%	Pl > Opx-CPx > Qz > Hbde-Bt
06MT37	14.6751	−61.0845	Piton du Carbet	Plateau Courbaril	Quartz and biotite bearing andesite	322 ± 9	30–45%	Pl > Opx-CPx > Qz > Hbde-Bt
06MT55	14.4705	−61.0548	Trois Ilets	Morne Clochette	Hyperstene bearing porphyritic andesite	1332 ± 30	30–50%	Pl > Px > Qz > Ox>Bt
06MT61	14.5070	−61.0620	Trois Ilets	Morne la Plaine	Clinopyroxene and olivine bearing basaltic andesite	1175 ± 20	10–15%	Pl > Px > Ol > Ox
18MT146	14.4682	−61.0755	Trois Ilets	Morne Jacqueline	Dioritic dike	~1000	100%	Pl > Px > Ox
06MT57	14.4971	−61.0860	Trois Ilets	Morne Champagne	Amphibole, plagioclase, biotite, porphyritic andesite	617 ± 52	30–40%	Pl > Px > Amp > Ox
06MT58	14.4965	−61.0873	Trois Ilets	Pointe Burgos	Quartz bearing basalt	N/A	15%	Pl > Px > Ox
06MT59	14.4656	−61.0516	Trois Ilets	Morne Larcher	Mega-plagioclase and quartz bearing andesite	346 ± 27	25–40%	Pl > Px > Qz > Ox>Bt
06MT28	14.8717	−61.1820	Mont Conil	Grand Riviere	Orthopyroxene and hornblende bearing andesite	543 ± 8	10–25%	Pl > CPx > Qz > Ox>Amp
09MT130	14.4920	−61.1113	Mont Conil	Piton Marcel	Orthopyroxene bearing andesite	126 ± 2	30%	Pl > Px > Ox
06MT51	14.8123	−61.1646	Mount Pelée	Dome 1902	Orthopyroxene bearing andesite	1902 CE	30%	Pl > Px > Ox
06MT50-I	14.8109	−61.1673	Mount Pelée	Dome 1929	Orthopyroxene bearing andesite	1929 CE	30%	Pl > Opx > Ox>Hbde

3.1. Definitions of plagioclase textures observed

Plagioclase crystals in studied samples exhibit various textures typical of remobilized antecrysts, along with phenocrysts and microlites. Textures of plagioclase crystals are used here to determine the remobilizing processes that occur in storage. In the samples studied, physical textures in plagioclase are classified into five categories (Fig. 3): (1) normal, (2) oscillatory, (3) resorbed core, (4) resorbed rim, and (5) sieved, which are all based upon previous classifications (Bennett et al., 2019; Renjith, 2014; Viccaro et al., 2010) and described below.

Type 1: Normal phenocrysts that grow in equilibrium with the melt and show normal to constant anorthite trends from core to rim (Fig. 3a), resulting in no apparent optical zoning (Renjith, 2014; Streck, 2008).

Type 2: An oscillatory texture is observed when a crystal exhibits 5–15 concentric zones (Renjith, 2014) (Fig. 3b). Oscillatory texture is caused by magma recharge when a new batch of magma is introduced into an existing magma chamber, which changes the chemical interface from the grain boundary and the melt (Renjith, 2014; Streck, 2008; Viccaro et al., 2010).

Type 3: Crystals with sieved texture contain random dissolution pockets of glass throughout the entire crystal (Renjith, 2014; Streck, 2008; Viccaro et al., 2010). Those melt inclusions can be sporadically distributed throughout the crystal (Fig. 3c), concentrated in the core (Fig. 3d), or in multiple or singular concentric bands (Fig. 3e). Sieved textures develop when crystals are remobilized and brought to shallower depths following the injection of a hotter, more primitive magma, into a resident crystal mush (Renjith, 2014; Viccaro et al., 2010).

Type 4: Resorbed core textures (Fig. 3f) show a subrounded to rounded skeletal core or irregular growths, resulting in a 'patchy' core surrounded by normal crystal growth around the outer rim of the core (Bennett et al., 2019). Resorbed cores develop after remobilization and decompression following the injection of a more mafic magma, but at slower rates and under water - saturated conditions compared to the processes responsible for the development of Type 3 texture (Viccaro et al., 2010).

Type 5: Resorbed rim textures (Fig. 3g) have subrounded external boundaries. Resorbed rims are formed when a mafic magma mixes with a more felsic crystal mush and remobilizes phenocrysts, allowing their boundaries to melt (Viccaro et al., 2010). If the intrusion is not immediately followed by an eruption, the remobilized resorbed crystals can grow further at equilibrium with the new melt, in which case the rim has a higher An content than the rest of the crystal.

Phenocrysts and microlites crystallize directly from the juvenile magma during ascent and eruption and show normal textures, whereas antecrysts formed from a cogenetic magma during previous magmatic stages and have been recycled by various magma replenishment events then incorporated into the final eruptive stage (Jerram and Martin, 2008). Crystals exhibiting texture Types 2–5 are considered antecrysts, which are the consequence of magmatic recycling, and are useful to better understand magmatic processes that occurred prior to eruption (Jerram and Martin, 2008).

3.2. Whole - rock geochemistry

All samples, except for 18MT146, were previously analyzed for whole-rock major elements, and details can be found in Germa et al. (2010, Germa et al., 2011a, 2011b) and in Labanieh et al. (2010). Sample 18MT146 was analyzed for major elements at the Center for Geochemical Analyses at the University of South Florida. After loss on ignition was measured on sample powders, flux fusion (modified after Murray et al., 2000) was conducted on 0.1 g of sample mixed with 0.4 g of $LiBO_2$ flux in a graphite crucible. Samples were heated to 1075 °C for 15 min until completely melted and then poured molten into a 50 mL of 2 M HNO_3 spiked with, and 10 ppm Ge used as an internal standard. The solutions were then diluted to 10,000× also into 2 M HNO_3 plus 10 ppm Ge solution to preserve the sample matrix. Calibration standards JB - 3,

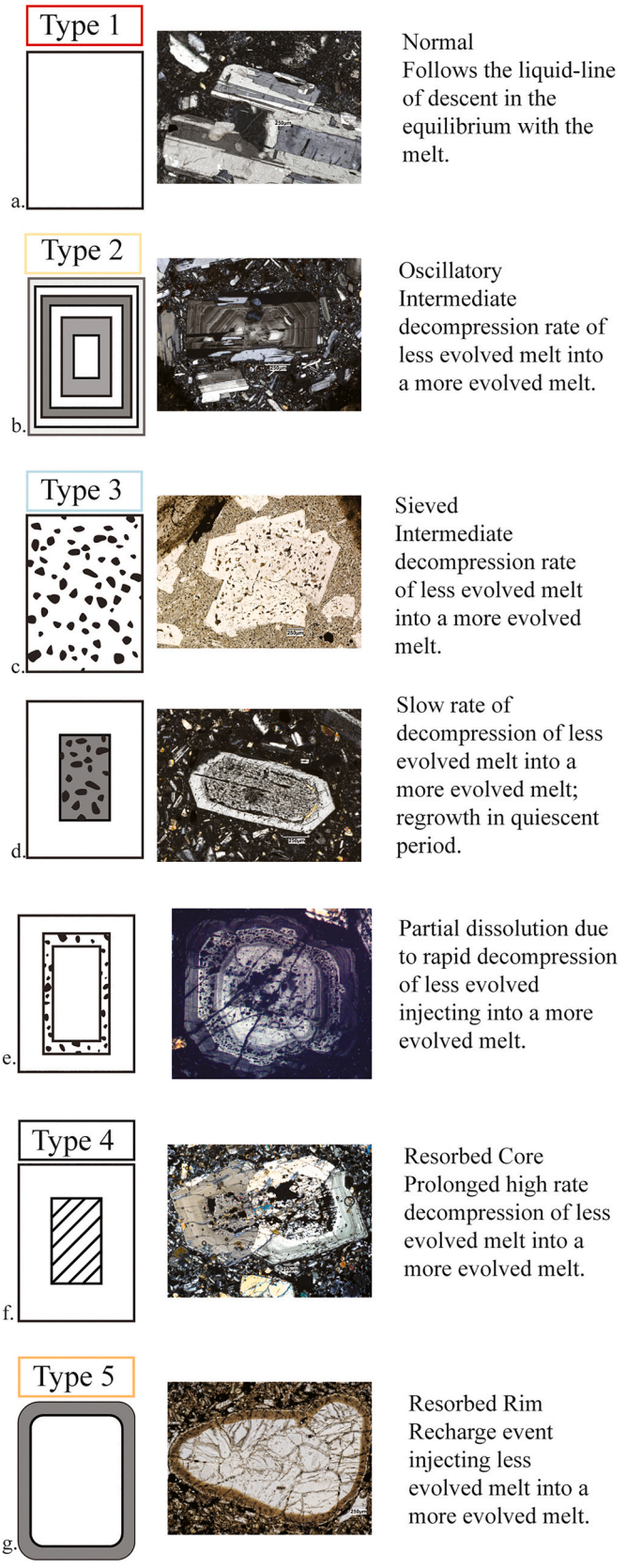

Fig. 3. Schematic representation of plagioclase textures and examples of crystals found in Martinique lavas.

JA - 2, and BHVO - 2 as well as internal standard JB - 3, JA - 2 were prepared identically and standard concentrations were adopted from the GeoReM database (Jochum et al., 2005). Solutions were analyzed using a Perkin Elmer 2000 DV Inductively Coupled Plasma Optical Emission Spectrometer (ICP - OES) with an analytical error of <5%. Published (Labanieh et al., 2010) and new whole - rock major element data is provided in Supp. Mat. 1 and Supp. Mat. 2.

3.3. Electron Probe Microanalysis

Carbon-coated thin sections were analyzed on a JEOL 8900R Superprobe at the Florida Center for Analytical Electron Microscopy (FCAEM) at Florida International University (FIU), Miami. Stage conditions were set with an accelerating voltage of 15 kV, a beam current set to 20 nA, and counting time of 10 s on peak for major elements. Data were corrected using a built in ZAF (atomic number, absorption, fluorescence) correction procedure. Standardization was completed on minerals in SPI standard blocks prior to analysis. The following standardswere used for primary calibration for each element. Si: Olivine, Plag An65, Augite, Muscovite and Alm - Garnet; Al: Muscovite, Augite, BHVO2 and Plag An65; Na: Plag AN65; MgO: Alm Garnet, Augite, Olivine and Biotite; K: Sanidine and Muscovite; Ca: Alm Garnet, Augite, Plag An65 and Diopside; Fe: Olivine, Muscovite and Alm. Garnet (https://case.fiu.edu/earth - environment/expertise/fcaem/). We selected microprobe chemical analyses that yielded totals between 97% and 103% and discarded data points with erroneous mineral structural formulae. EPMA data is reported in Supp. Mat. 1 for plagioclase and Supp. Mat. 2 for pyroxene.,

3.4. Thermobarometers

To constrain crystal-liquid equilibrium pressures (P) and temperatures (T), we applied mineral-melt equilibria geobarometers and geothermometers described in Putirka (2008). We paired clinopyroxene, orthopyroxene, and plagioclase with whole-rock compositions representing the initial crystal-free melts. As recommended by Putirka (2008), FeO wt% was converted from Fe_2O_3 wt% to FeOt using eq. (1).

$$FeO_t = Fe_2O_3\,(wt.\%) \times 0.8998 \quad (1)$$

3.4.1. Plagioclase – liquid thermometer and hygrometer

We calculated the dissolved H_2O wt% in the melt using Lange et al. (2009) plagioclase - liquid hygrometer. To calculate plagioclase-liquid equilibrium temperatures, we used eq. 23 from Putirka (2005), using whole-rock data and H_2O wt% to link crystal cores to liquid compositions. Results were validated using the recommended test for equilibrium with a partition coefficient of K_D (An - Ab)$^{plag\text{-}liq}$ 0.10 ± 0.05 for temperatures below 1050 °C, and of 0.28 ± 0.11 for temperatures higher than 1050 °C (Putirka, 2008). Crystal cores with K_D (An - Ab) $^{plag\text{-}liq}$ outside of this range were not used in plots or in the discussion, but results are included in Supp. Mat. 1 for reference. In the absence of satisfactory glass compositions for our samples, we have tested pairing rims with whole-rock data. As expected, most rims are out of equilibrium with whole-rock compositions and are therefore omitted from our results and discussions. Plagioclase-liquid temperatures, anorthite compositions, H_2O wt%, plagioclase components, and K_D (An - Ab) $^{plag\text{-}liq}$ are reported in Supplementary Material 1 along with EPMA data and whole - rock major elements used as input.

3.4.2. Pyroxene-liquid thermobarometers

We used clinopyroxene-liquid and orthopyroxene-liquid thermobarometers from Putirka (2008) to calculate temperature, pressure, Mg#, predicted and observed components and their sums, and Fe - Mg exchange coefficient K_D (Fe - Mg) $^{pyrx\text{-}liq}$. Specifically, we used eqs. 29a for pressure and 28a for temperature from the orthopyroxene-liquid thermobarometer, and eq. 33 for temperature and eq. 31 for pressure from the clinopyroxene-liquid thermobarometers. In the absence of satisfactory glass compositions for our samples, we have paired core data points with whole-rock data, using dissolved H_2O wt% content calculated with Lange et al. (2009) as described above. Samples were considered at equilibrium if their Fe - Mg exchange coefficient was within 0.29 ± 0.06 for orthopyroxene and 0.28 ± 0.08 for clinopyroxene (Putirka, 2008). However, as K_D (Fe - Mg) $^{pyrx\text{-}liq}$ is not always a reliable indicator of equilibrium for a range of compositions (Putirka, 2008), we also used the difference between diopside and hedenbergite components predicted for clinopyroxenes (DiHd) (Supp. Mat. 2), and the predicted component sums as close to 1 as possible (Putirka, 2008). Results, Rhodes diagrams, and tests for equilibrium are reported in Supplementary Material 2 along with EPMA data and whole - rock major elements used as input. Using pyroxene pressure estimates, we calculated depths of storage using eq. (2):

$$D = \frac{P}{\rho g} \quad (2)$$

with D the depth in meters, P the pressure in Pa, g the acceleration due to gravity (9.81 $m.s^{-2}$), and ρ the average LAIA crustal density of 2600 kg. m^{-3} (Christeson et al., 2003). Finally, data points that show a crystal - liquid equilibrium deeper than 40 km were rejected, based on the crustal model proposed by Melekhova et al. (2019) that suggest Moho depths ≤32 km. Depths are reported in Supplementary Material 2 along with calculated absolute uncertainty Δx for each individual parameter (x_i) after Taylor (1997).

3.4.3. Error propagation

We calculated the absolute uncertainty Δx for each individual parameter (x_i) as described in Taylor (1997).

We first calculated the mean of the parameter as:

$$\overline{x} = \frac{\sum x_i}{N} \quad (3)$$

With x_i being either temperature, pressure, anorthite, or water content, and N the total number of data points.

Then, we calculated the standard deviation σ_x (as)

$$\sigma_x = \sqrt{\frac{\sum (x_i - \overline{x})^2}{N-1}} \quad (4)$$

Finally, the absolute uncertainty is calculated as:

$$\Delta x = \frac{\sigma_x}{\sqrt{N}} \quad (5)$$

and expressed with the same unit as the parameter it is associated with.

4. Results

4.1. Petrography and plagioclase textural diversity

4.1.1. Morne Jacob

Sample 06MT34, from Pain de Sucre lava flow (Fig. 1b and, Table 1) is a porphyritic basaltic andesite with 5 to 15% vol. of crystals. The main mineral phase is plagioclase (92%), with crystal sizes ranging between 200 μm to >2 mm, and accessory minerals consist of augite (3%) and oxides (5%) with grains <1 mm. Phenocrysts are surrounded by a microcrystalline groundmass of plagioclase and clinopyroxene. Normal (43%) and sieved (53%) plagioclase textures dominate (Fig. 4). Sample 06MT10, from Morne Bellevue lava flow (Fig. 1b and Table 1) is a porphyritic andesite with 20 to 40 vol% of crystals. The main mineral phase is plagioclase (75%, 100 μm - 1 mm), associated with two pyroxenes (hypersthene and augite, 20%, 100–500 μm) and oxides (5%). Normal (43%), resorbed rim (32%), and sieved (18%) textures dominate the plagioclase cargo (Fig. 4).

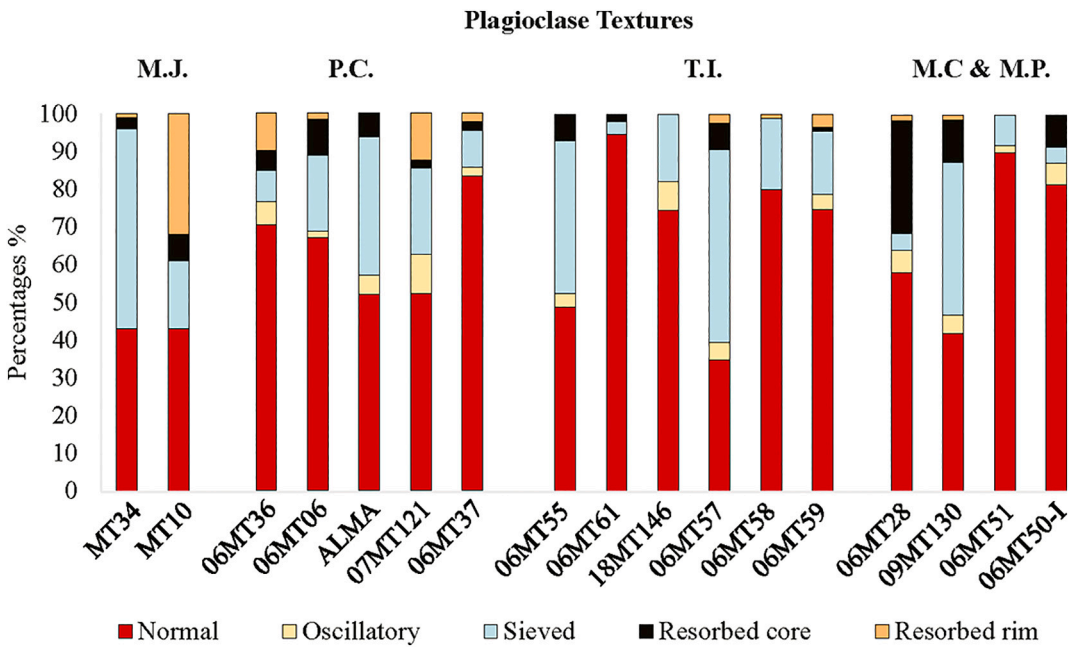

Fig. 4. Frequency of plagioclase crystal textures counted for each sample: normal (red), oscillatory (yellow), sieved (blue), resorbed core (black), and resorbed rim (orange). Acronyms: M.J. (Morne Jacob 4101 ± 60–2111 ± 30 ka), P.C. (Pitons du Carbet 998 ± 14–331 ± 6 ka), T.I. (Trois Îlets 1332 ± 30–346 ± 27 ka) M.C. & M. P. (Mt. Conil – Mt. Pelée 543 ± 8–1929 CE). (For interpretation of the references to color in this figure legend, the reader is referred to the web version of this article.)

4.1.2. Pitons du Carbet complex

Overall, samples from the Pitons du Carbet complex are light gray porphyritic andesites and dacites. Rocks have a 30–45 vol% of crystals with sizes ranging between 0.1 and 20 mm. Two samples, Piton Gelé (06MT06, Fig. 1b, and Table 1), and Morne Césaire (06MT36, Fig. 1b, and Table 1) lava domes belong to the first eruptive phase. They contain plagioclase (80–70%), orthopyroxene (5%), quartz (10%) and some hornblende (10–1%). Three samples belong to the second eruptive phase, or Pitons du Carbet sensu stricto, a group of lava domes and flows emplaced inside the horseshoe shaped depression just after the collapse (Fig. 1b and Table 1). These samples are from Piton Boucher lava dome (07MT121), Piton de l'Alma lava dome (Alma), and Plateau Courbaril lava flow (06MT37). Samples have both orthopyroxene and clinopyroxene (1–3 mm) and are also characterized by the occurrence of large (4–7 mm) crystals of hornblende and biotite, and a larger amount of quartz (up to 7 mm). Interestingly, samples from both stages contain a majority of plagioclase with normal textures, and a slight increase in the fraction of sieved and oscillatory textures can be seen for the younger samples (Fig. 4).

4.1.3. Trois Îlets volcanic field

Samples from the early eruptive cycle of Trois Îlets volcanic field include (Fig. 1b and Table 1) Morne Clochette (06MT55), Morne La Plaine (06MT61), and a dioritic dike from Morne Jacqueline (18MT146). Morne Clochette consists of a hypersthene bearing andesite with a crystallinity of 30–50% vol. and a mineral mode of plagioclase (70%), pyroxene (25%), quartz (1%), oxide (2%), and biotite (1%). Texturally, the rock contains phenocrysts (70% of crystals, up to 3 mm) in a cryptocrystalline matrix. Morne la Plaine lava flow is an olivine and clinopyroxene bearing basalt with a crystallinity of 10–15% vol. Mineral mode includes plagioclase (81%), pyroxene, (15%), olivine (2%), and oxide (2%). A dioritic dike (sample 18MT146) from Morne Jacqueline contains phenocrysts of plagioclase (80%), pyroxene (15%), and oxide (5%) in a cryptocrystalline groundmass. All samples from this first eruptive cycle contain plagioclase with normal textures in majority (>50%), with a few sieved crystals, oscillatory textures, and resorbed cores (Fig. 4). Three samples were selected from the late eruptive cycle along a NW - SE volcanic alignment (Fig. 1b, Table 1). Sample 06MT57 (Morne Champagne lava dome) is an amphibole bearing andesite with 30–40% vol. crystals of plagioclase (50%), pyroxene (42%), amphibole (5%), and oxide (3%). Pointe Burgos (sample 06MT58) is a basaltic - andesite with plagioclase (43%), pyroxene (50%), oxide (2%), and xenocrysts of quartz (5%). Quartz xenocrysts (up to 5 mm) are highly fractured and may have been picked up upon magma ascent or result from secondary recrystallization (Westercamp et al., 1989). Sample 06MT59 from Morne Larcher dome complex is a porphyritic (25–40 vol % crystals) andesite with plagioclase (75%) pyroxene (22%), quartz (2%), and oxide (1%). In the recent samples, normal plagioclase textures dominate, but we see an increase in sieved, oscillatory, and resorbed cores crystals compared to samples from the first phase (Fig. 4).

4.1.4. Mt. Conil and Mt. Pelée

Sample 06MT28 belongs to the oldest part of Mt. Conil. It is a dark porphyritic (10–25% vol. crystals) andesite rich in plagioclase (85%), clinopyroxene (7%), quartz (3%), oxide (5%), and rare amphibole. Plagioclase crystals display normal (58%) and resorbed core (30%) textures, and a minority of crystals with oscillatory or sieved textures (Fig. 4). t.

Sample 09MT130 is a light fine-grained andesite collected from Piton Marcel, a lava dome emplaced just after the first flank collapse (126 ka, Germa et al., 2011b, Fig. 1b, and Table 1). Plagioclase is the main mineral (65%), followed by pyroxene (30%), and oxide (5%). Normal (42%) and sieved (41%) plagioclase textures dominate (Fig. 4). T Sample 06MT51 (c.e. 1902 dome) is an orthopyroxene bearing andesite, consisting of plagioclase (70%), pyroxene (25%) and oxides (5%). Normal (90%) and sieved (8%) plagioclase textures are observed (Fig. 4). Mt. Pelée's 1929 lava dome (sample 06MT50) is a fine - grained light andesite, with plagioclase (80%), orthopyroxene (10%), oxides (5%) and hornblende (5%). Plagioclase textures are mostly normal (82%), oscillatory (6%), and resorbed cores (9%) (Fig. 4).

4.2. Plagioclase chemistry and thermometry

Overall, plagioclase compositions range from An_{47} to An_{86}, with some compositions as low as An_{31} and as high as An_{96} (Fig. 5a) and can be classified as calcic andesine to sodic bytownite with minimal

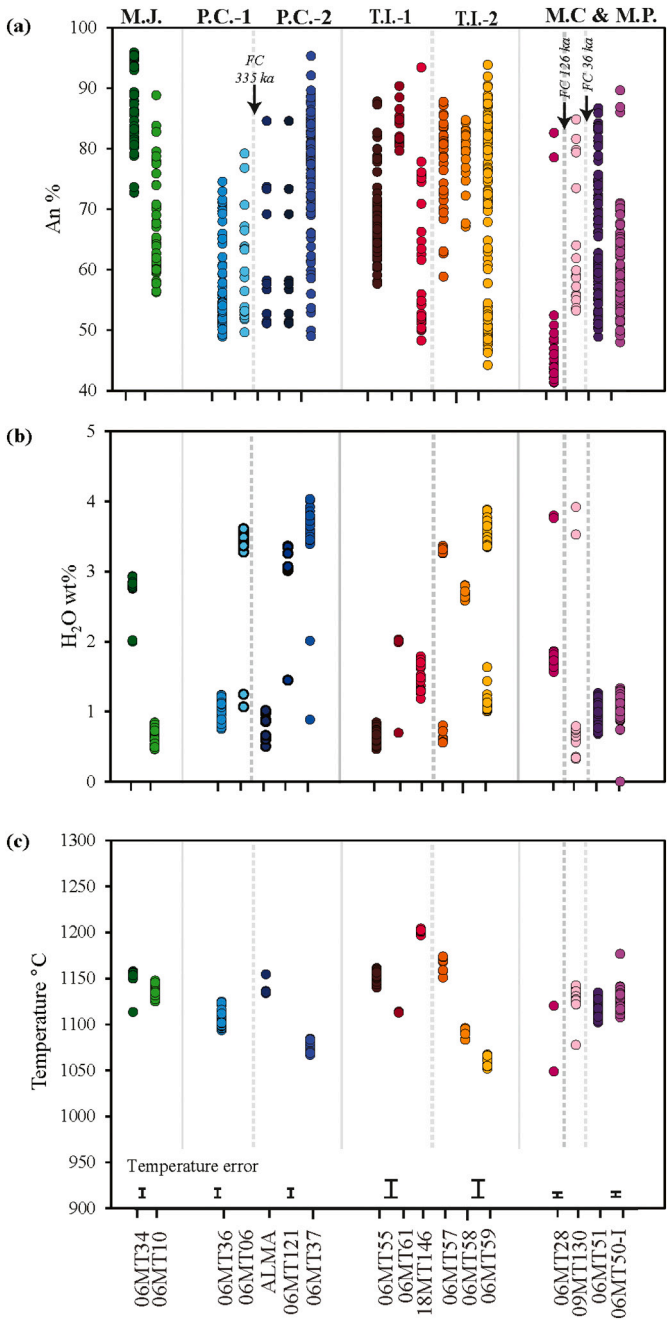

Fig. 5. (a) Anorthite compositions, (b) plagioclase-liquid temperatures, presented here are from data points that are in equilibrium with the melt, with error bars calculated per complex, and (c) melt water content calculated from plagioclase using Lange et al. (2009). Each circle represents an individual data point. Acronyms at the top of 5(a) indicate the name of the volcanic complex. For Morne Jacob (M.J.) [4101 ± 60–2111 ± 30 ka], Pitons du Carbet complex phase 1 (P.C.-1) [998 ± 14–770 ± 11 ka], Pitons du Carbet complex phase 2 (P.C.-2) [338 ± 5–331 ± 6 ka], Trois Îlets field first eruptive cycle (T.I.-1) [1332 ± 30 - ~1000 ka], Trois Îlets volcanic field second eruptive cycle (T.I.-2) [617 ± 52 - ~346 ka], and Mt. Conil – Mt. Pelée (M.C. & M.P.) [543 ± 8 ka - 1229 CE].

orthoclase content (<Or_2). Samples from Morne Jacob show the widest range of plagioclase compositions, with compositions mostly of An_{55} – An_{95} (Fig. 5, Table 2). However, the youngest sample contains more sodic compositions compared to the old one (Fig. 5a). There is a clear dichotomy between the pre- and post-collapse samples from Pitons du Carbet complex (Fig. 5a). Indeed, samples from the first phase contain mostly sodic labradorite compositions (~An_{50} – An_{70}), while the second phase has more calcic plagioclase that classify as bytownite (An_{50} – An_{90}). Plagioclase compositions from Trois Îlets volcanic field display a tri-modal distribution, with compositions mostly of An_{45}-An_{56}, An_{60}-An_{65}, and An_{70}-An_{85} (Fig. 5, Table 2), which can be explained by the distributed nature of the volcanic vents. Finally, Mt. Conil – Mt. Pelée complex contains plagioclase that classifies mostly as labradorite (An_{50}-An_{65}) and bytownite (An_{70} An_{90}) However, the anorthite compositions seem to gradually increase toward recent samples erupted after the 126 ka flank collapse (Fig. 5a).

Dissolved water calculated from plagioclase compositions (Lange et al., 2009) show a bi-modal distribution, with values between 0.3 and 1.4 wt% and between 3.2 and 4.0 wt% overall (Fig. 5b). This duality is seen for Morne Jacob samples, Pitons du Carbet complex, and Trois Îlets volcanic field (Table 2 and Fig. 5). Specifically, the first stage of Morne Jacob contains more dissolved water than the recent one. The opposite is true for Pitons du Carbet complex for which the second phase is more hydrated (3.0–4.1 wt%) than the first. Samples from the early phase of Trois Îlets volcanic field contain dissolved water under 2 wt%, whereas the recent samples can have up to 4 wt% of H_2O (Fig. 5b, Table 2). Finally, the samples erupted after the 126 ka collapse contain less water (<2 wt%) than the old ones (>1.5 wt%, Fig. 5, Table 2).

Out of 719 plagioclase analyzed by electron microprobe, 326 are within the recommended $Kd(Ab\text{-}An)^{plag\text{-}liq}$ and therefore are considered to be at equilibrium with the whole-rock composition used for plagioclase-liquid thermometer. Indeed, antecrysts, especially those with oscillatory textures and those showing evidence of multiple remobilization events, may have grown from different magma batches, and therefore will not be considered at equilibrium with the liquid used in the calculations. Consequently, only data points at equilibrium with whole-rock compositions are used here. Overall, all four volcanic complexes considered, the feldspar-liquid geothermometer yielded a temperature range of 1052–1204 °C, with ±2 °C absolute uncertainties and a median of 1124 °C. More specifically, we calculated average temperatures of about 1140.1 °C ± 1.5 °C for Morne Jacob, 1098.3 ± 1.7 °C for Pitons du Carbet complex, 1151.6 ± 3.5 °C for Trois Îlets volcanic field, and 1120.2 ± 1.3 °C for Mt. Conil – Mt. Pelée (Table 2, Fig. 5c). Trois Îlets volcanic field displays multiple temperature clusters specific to each sample, whereas the other complexes seem to display more restricted ranges.

4.3. *Pyroxene chemistry and thermobarometry*

Out of 38 clinopyroxene-liquid pairs analyzed, 24 are within the Kd $(Fe—Mg)^{cpx\text{-}liq}$ range of 0.28 ± 0.08 recommended to test for equilibrium. The more robust DiHd test for equilibrium shows that all the cpx-liquid pairs approach the equilibrium of the model (Supp. Mat. 2). The orthopyroxene phases present in our samples show a range in KD $(Fe—Mg)^{opx\text{–}liq}$ from 0.34 to 1.03, and all but one data point are outside the recommended range of 0.29 ± 0.06, suggesting that the orthopyroxene data is out of equilibrium with the melt (Supp. Mat. 2). The Mg numbers of our orthopyroxene range from 39 to 76, about the same as predicted from the host melt composition (39–65), but plot outside the range for equilibrium in a Rhodes diagram (Supp. Mat. 2). Consequently, we are considering the pressures and temperature calculated from OPx-liquid pairs with caution as first approximations only.

The clinopyroxene-liquid geothermobarometer, with ±10 °C and 0.3 kbar uncertainties, yielded temperatures between 802 and 1170 °C and a pressure range of 1.5 to 9.7 kbar overall. The orthopyroxene-liquid geothermobarometer yielded a temperature range of 884 to 1060 °C with an absolute uncertainty of 3 °C; and pressures between −1.3 and 4.5 kbar with absolute uncertainty of 0.1 kbar. Temperatures and pressures for individual complexes, and their errors are summarized in Table 2, and details can be found in Supp. Mat. 2. Overall, most of the samples show crystallization from the mantle to the surface. A higher frequency of points indicates preferential storage at the Moho, in the

Table 2
Range of calculated crystal - liquid equilibrium geobarometers, geothermometers, and hygrometer using Putirka (2005, 2008), Lange et al., 2009, and Germa et al., 2010; Germa et al., 2011a, 2011b.

Sample	Plag				Opx					Cpx				
	An	T(°C)	± ΔT°C	H2O (wt %)	T (°C)	± ΔT°C	P(kbar)	± ΔP (kbar)	Depth (km)	T (C°)	± ΔT°C	P (kbar)	± ΔP (kbar)	Depth (km)
		Putirka (2005)		Lange et al., 2009	Putirka (2008)					Putirka (2008)				
		Eq. 23			Eq. 28a		Eq. 29a			Eq. 33		Eq. 31		
Morne Jacob														
06MT34	73–96	1080–1292		2.00–2.94										
06MT10	56–89	1125–1158		0.46–0.85	1014–1025	2.25	0.8–2.4	0.19	3 - 10	979–1050	10.31	1.5–9.0	1.12	6 - 35
Pitons du Carbet														
06MT36	49–75	1094–1130		0.75–1.24	896–966	4.71	1.6–3.3	0.11	6 - 13					
06MT06	50–79	1027–1137		1.07–3.61	957–962		0.20–0.24		8 - 9					
ALMA	51–85	1122–1167		0.51–1.02	961		2.5		10	1013–1034	10.28	6.7–6.9	0.36	26–27
07MT121	51–85	1040–1123		1.45–3.36						995–1016		6.0–9.0		23–35
06MT37	49–95	1040–1156		0.89–4.04	933		2.5		10	1078		4.3		17
Trois Ilets														
06MT55	58–88	1140–1175		0.47–0.85	1003–1036	5.5	0.4–1.8	0.77	2 - 7	1003–1053	14.19	7.2–9.7	0.45	28–38
06MT61	80–90	1093–1115		0.71–2.03	1036		5.6		22	1167–1171		7.1–7.4		28–29
18MT146	48–93	1152–1210		1.19–1.79										
06MT57	59–88	1058–1174		0.56–3.37										
06MT58	67–85	1083–1099		2.59–2.80						1089–1130		2.3–6.9		9 - 27
06MT59	31–94	1039–1154		1.00–3.88	1019–1037		0.5–2.2		2 - 9	1039–1074		4.6–7.1		18–28
Mt. Conil - Mt. Pelee														
06MT28	41–83	1049–1120		1.57–3.80						1053	0	6.1	0	24
09MT130	0.33–3.92	1047–1163		0.33–3.92	970–992	1.51	−2.7	0.12	1 - 3					
06MT51	49–87	1102–1150		0.68–1.27	947–1002		−2.8		0 - 6					
06MT50-I	48–90	1045–1177		0.00–1.34										

upper crust, and in the shallowest volcano-sedimentary layer (Fig. 6e). Morne Jacob magmas crystallized in storage regions located at the base of the lower crust and in the upper crust, with no apparent storage in the lower or middle crust (Fig. 6a). Samples from the first phase of Pitons du Carbet containing only OPx, indicate storage in the upper crust (Fig. 6b). Post-collapse samples indicate crystallization from the mantle all the way to the top of the lower crust, as well as in the upper crust, with an outlier in the middle crust. Interestingly, all the deep samples indicate adiabatic crystallization at about 1050° from about 35 to 25 km (Fig. 6b). Trois Îlets volcanic field is the only field with transcrustal crystallization from ~39 km all the way to the surface. However, each edifice within this field is fed by distinct magma batches from different storage depths. For instance, the Morne Clochette lava flow (sample 06MT55) shows magma storage conditions from the mantle, lower crust, and upper crust. The Morne La Plaine basaltic lava flow (06MT61) only shows magma storage conditions at the Moho. The Pointe Burgos basalt (06MT58) is fed by magma that crystallized through the lower crust and then adiabatically through the middle and upper crust (Fig. 6d). Finally, the absence of good CPx data points for the old phase of Mt. Pelée, prevents us to obtain significant storage conditions in the crust for this edifice, except for the shallowest volcano-sedimentary layer. Although OPx thermobarometry results are out of equilibrium, the depths and temperatures obtained are consistent with those found in the literature, with depth < 6 km and temperatures of about 950–1000 °C (Martel et al., 2006; Pichavant et al., 2002).

5. Discussion

5.1. Magma storage conditions in Martinique in the last 5.5 Ma

Samples from the recent volcanoes of Martinique show crystallization at various depths within the crust, with location of magma bodies that vary spatially and temporally (Fig. 6). The most frequent crystallization depths are found in the shallowest crust (<2 km), at the base of the upper crust (6–10 km), at the Moho (Fig. 6). There is limited storage in the middle-crust for most complexes (Fig. 6e). Specifically, samples from the recent Mt. Pelée indicate crystallization in the last 6 km beneath the surface, and agrees well with previous studies (Annen et al., 2008; Fichaut et al., 1989; Gourgaud et al., 1989; Martel et al., 1998; Smith and Roobol, 1990; Traineau et al., 1983). The dacites from Piton du Carbet contain crystals that formed at 16–35 km (lower crust) and 6–13 km (upper crust). These are consistent with an earlier study that suggested depths of 8–16 km (Coulon et al., 1984; d'Arco et al., 1981).

Overall, our results agree well with previous depths and magma temperatures calculated for Mt. Pelée and Pitons du Carbet in Martinique (Metcalfe et al., 2023, and references therein). However, our enlarged dataset that includes older volcanoes from the recent arc shows that storage regions also exist as deep as in the lower crust and the mantle beneath Martinique. Indeed, the deepest reservoirs for this island were previously thought to be no deeper than ~15 km in the middle crust (Metcalfe et al., 2023). Nevertheless, such a multi-level magma plumbing architecture is remarkably similar to that suggested at other volcanoes along the Caribbean coast of the Lesser Antilles islands (Fig. 2a; Metcalfe et al., 2023; Balcone-Boissard et al., 2023). Recent volcanoes have vertically extensive plumbing systems from (>35 km depth to the surface), although magmas of various compositions are

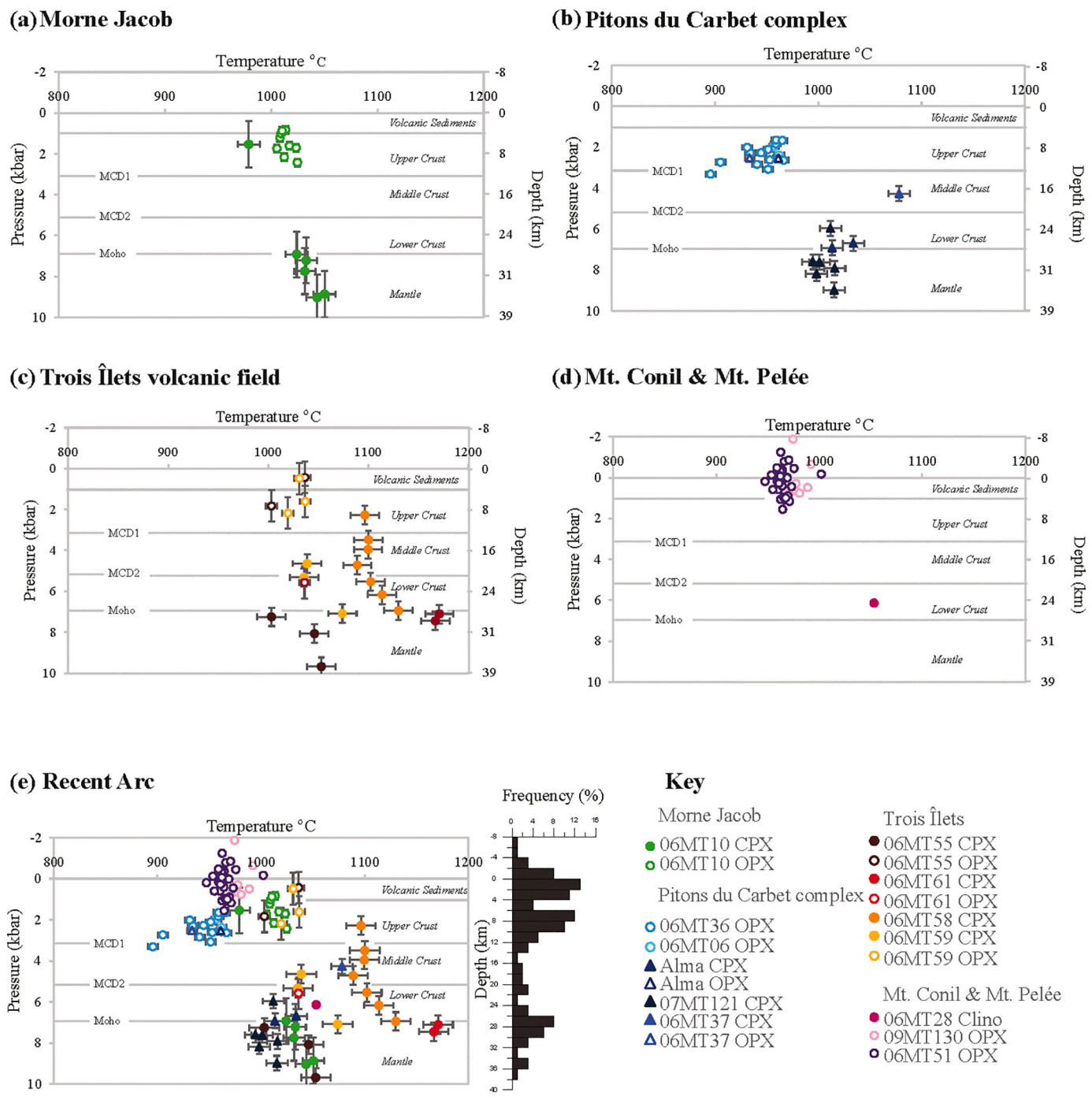

Fig. 6. Pyroxene-liquid temperatures and pressures calculated from orthopyroxene (open circle) and clinopyroxene (closed circle) using Putirka (2008) model. All data points have a corresponding temperature and pressure error bars. (a) Morne Jacob – (sample 06MT10). (b) Pitons du Carbet complex (samples 06MT36, 06MT10, Alma, and 07MT121). (c) Trois Îlets volcanic field (samples 06MT55, 06MT61, 06MT58, 06MT59, and 18MT144). (d) Mt. Conil & Mt. Pelée (samples 06MT28, 09MT130, 06MT51, and 06MT50 – I). Superimposed on the P-T graphs is the crustal model of Melekhova et al., 2019 containing volcanic sediments, upper crust, MCD1, middle crust, MCD2, lower crust and mantle.

stored at different depths (Balcone-Boissard et al., 2023; Camejo-Harry et al., 2019; Camejo-Harry et al., 2018; Christopher et al., 2015; Cooper et al., 2016; Edmonds et al., 2016; Metcalfe et al., 2023; Melekhova et al., 2019; Melekhova et al., 2017; Stamper et al., 2014; Ziberna et al., 2017). These studies also show magma focusing preferentially within specific crustal layers and at mid-crustal discontinuities, while some other crustal regions do not seem to promote magma storage (Metcalfe et al., 2023; Balcone-Boissard et al., 2023). Apart from the deep storage region that is common to all islands, the depths of the storage regions are generally within the middle to upper crustal layers, with most storage constrained to 5 to 8 km depth within low-density crustal layers (Melekhova et al., 2019), and at mid-crustal discontinuities where density contrast between layers is sharp (Kavanagh et al., 2006; Maccaferri et al., 2010). Overall, the depth and extent of the main andesitic to dacitic magma bodies vary beneath each island, with persistent silicic magma chambers that feed eruptions located in the upper crustal layer (< 5 km).

Overall, the storage temperatures calculated in this study range in

the upper half of the Lesser Antilles magmatic temperatures (Fig. 2b). Temperatures between 750 °C and > 1300 °C have been reported at other volcanoes from a large variety of sample types (hard samples from lava flows and domes, tephra, xenoliths) and various methods (melt inclusions, whole-rock, crystals). Note that our samples are exclusively from lava flows and domes, with a majority of basaltic-andesites and andesites. Nevertheless, the range of storage temperatures calculated for individual complexes agree well with found in the literature for Mt. Pelée, Pitons du Carbet complex, and other Lesser Antilles volcanoes (Metcalfe et al., 2023; Balcone-Boissard et al., 2023). Interestingly, the central Lesser Antilles islands yield some of the highest storage temperatures and pressures in the whole arc (Fig. 2). This could be related to a local increase of heat flux, magma production, or simply recurrent magma batches that are close in space and time (Germa, 2009; Higgins and Caricchi, 2023). Higher magma fluxes might be related to core complexes that have higher water content in the subducting lithosphere due to localized serpentinized mantle, generally along fracture zones (Cooper et al., 2020; Higgins and Caricchi, 2023) and could explain the higher magma temperatures found for these islands (Fig. 2b).

5.2. Evolution of Martinique volcanoes

5.2.1. General evolution through time

Chemistry and physical textures in all samples indicate that multiple recharge events by injection of basaltic to basaltic - andesite magmas frequently remobilized crystal mushes, inducing variable decompression rates, mechanical mixing, resorption of remobilized phenocrysts, and further crystallization in shallow storage conditions. We propose that the plumbing systems of volcanoes in Martinique evolve from a simple deep storage system to a more extensive system consisting of distinct shallow reservoirs in multiple crustal layer, extending all the way to the surface, allowing for magma differentiation, mixing, and crystal remobilization (Fig. 7a). As an edifice develops, the superficial load progressively prevents mafic magma from erupting (Pinel and Jaupart, 2000), and storage and differentiation progress toward shallower depths, as indicated by polybaric crystallization paths (Fig. 6e). Overall, throughout the history of each volcano, eruptions were fed from two distinct magma regions, one of basaltic-andesite to andesitic composition stored at 7–12 km and 900–1050 °C, and another one of andesitic to dacitic composition above 2 kbar (6 km). This is consistent with similar processes proposed for Mt. Pelée (Annen et al., 2008; Boudon and Balcone-Boissard, 2021; Gourgaud et al., 1989; Martel et al., 1998; Pichavant et al., 2002). The reservoirs in the upper crust are fed by basaltic and basaltic-andesite magmas originating from the mantle and lower crust, with temperatures of 1000 °C – 1150 °C (Bourdier et al., 1985; Martel et al., 1998; Pichavant et al., 2002). Several studies suggested that the Mt. Pelee shallow magma chambers are vertically elongate reservoirs based on petrography, geochemistry, and experimental data (Fichaut et al., 1989; Pichavant et al., 2002; Metcalfe et al., 2023). At Morne Jacob, Pitons du Carbet, and Mt. Conil – Mt. Pelée, the young samples generally contains all five plagioclase texture types, sometimes with two or more textures over imposed in single crystals, suggesting

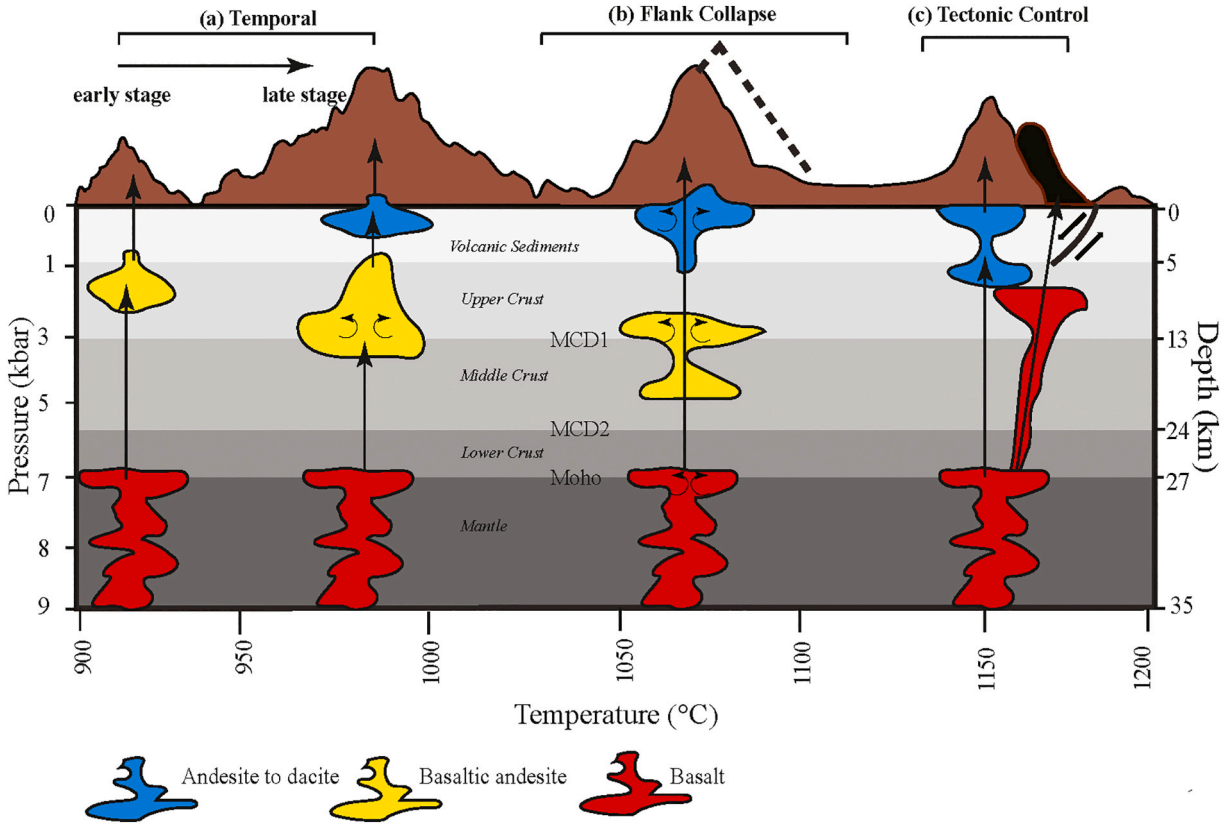

Fig. 7. Conceptual model of Martinique plumbing systems and their evolution with time or surface morphological changes.
(a) Temporal evolution: basaltic magmas intrude the lower crust and evolve toward basaltic andesite compositions. Magmas then can ascend toward the upper crust with minimal storage in the middle crust. If storage develops in the middle crust, magmas pond at the deepest mid-crustal discontinuity. Andesitic to dacitic magmas are stored and evolve in the upper crust, from which they feed eruptions. Often, mafic magmas ascending from the lower crust will remobilize the shallow crystal mushes and trigger eruptions.
(b) Flank collapse. The sudden decompression due to rapid unloading at the surface induced by a flank collapse allows deep mafic magmas to ascend and remobilize shallow crystal mushes rapidly, with rapid volatile exsolution.
(c) Tectonic control: shallow faults and crustal fractures promote quick magma ascent with minimal storage in the crust. This prevents magmatic reservoirs to develop and promotes distribution of melts in the subsurface, explaining the distinct geochemical signatures observed at individual volcanoes.

antecrysts are remobilized from various magma lenses by frequent injection of basaltic melts (Higgins et al., 2021; Neave and Putirka, 2017). Such variety is generally not observed in old samples and suggests that complexity in the architecture of plumbing systems develops over time. However, storage conditions and compositions for Trois Îlets Volcanic field, Pitons du Carbet complex, and Mt. Conil – Mt. Pelée show more complex trends that suggest the influence of external factors, mostly due to the existence of structural and tectonic systems.

5.2.2. Trois Îlets volcanic field

Trois Îlets Volcanic field shows a spatio-temporal trend different from the other recent volcanoes in Martinique. Samples systematically exhibit the highest storage temperatures and have the widest temperature range (Table 2, Fig. 2b). Our results indicate that eruptions are fed from distinct magma batches that originate from different crustal depths and different magmatic temperatures (Figs. 5 and 6). Each magma batch has a singular composition (Germa et al., 2011, Labanieh, 2009) and water content (Fig. 5c).

Indeed, volcanoes of Trois Îlets are small-volume edifices distributed over a small area (<50 km^2, Fig. 1b) and appear to have distinct plumbing systems (Germa et al., 2011b). Indeed, volcanoes are spatially distributed, without evidence of a central system, and each display distinct petrographic characteristics. Interestingly, there seems to be a change in the architecture of plumbing systems through time beneath Trois Îlets volcanic field. Indeed, thermobarometry data from the oldest samples (05MT55 and 06 M61) reveal that magma ponds at the Moho and within the lower crust where clinopyroxene crystallize around 6–8 ± 0.4 kbar (25–32 km) at temperatures of 1017–1060 °C. Orthopyroxenes crystallize closer to the surface (0.13 kbar or 0.5 km) within the upper crust at temperatures of 1074 °C (Fig. 6c). Therefore, there is a crystallization gap between ~25 km and the upper crustal layer (~3 km), indicating limited to no magma storage and crystal growth in the lower and middle crust (Fig. 6c). In contrast, samples from the second eruptive cycle (06MT57, 06MT58, 06MT59, and 18MT146), all younger than 600 ka, present more complex mineral assemblages that crystallized through multiple lenses stored at various depths from the lower to the upper crust (Fig. 6c). Previous geologic investigations suggested the presence of numerous faults and fractures within the Trois Îlets volcanic field (Gadalia et al., 2014; Germa et al., 2011b; Westercamp et al., 1989), which may have favored a relatively fast ascent of mafic magmas toward shallow depth (Fig. 7c). Plagioclase in Trois Îlets samples have a large proportion of sieved textures suggesting a fast decompression rate. Also, the basaltic lava flow of Morne La Plaine (sample 06MT61) contains large (up to 3 mm) olivine crystals (1%) supporting ascent of mafic magma carrying olivine phenocrysts. Samples analyzed in this study contain virtually no textures related to frequent remobilization events or magma mixing (Fig. 4). These results let us argue that the structure of the crust or the frequency of magma batches beneath Trois Îlets volcanic field do not promote magma focusing toward a central vent, and do not enhance mixing of magma batches as observed for the other volcanoes.

5.2.3. The Pitons du Carbet complex

The Pitons du Carbet complex lies above the western flank of Morne Jacob volcano.

Phase 1 samples (06MT36, 06MT06) show a complex assemblage of plagioclase textures, with a dominant oscillatory and reverse anorthite compositional pattern from core to rim, and plagioclase are mostly sodic labradorite (Supp. Mat. 3). Textures also display dissolution pockets, resorption surfaces, and zoning (Supp. Mat. 3). Overall, during the first eruptive cycle, cold dacitic magmas are stored in a shallow storage region, and crystal mushes often remobilized by injection of magmas ascending from the mantle (Fig. 7a). After the flank collapse (337 ± 3 ka, Germa et al., 2011b), the crystal record indicates that magma crystallizes not only in the upper crust, but also in the lower crust (Figs. 6b and 7b). Plagioclase ($An_{47–98}$) yields temperatures between 1067 °C and 1155 °C, and 3–4 wt% H_2O (Fig. 5). Lavas that erupted after the flank collapse contain both clino- and orthopyroxene and suggest that magmas that fed the post-collapse eruptions samples crystals from the lower and the upper crust, whereas magmas that fed pre-collapse eruptions only samples upper crustal reservoirs.

Additionally, whole - rock major elements (Germa et al., 2011b) show that the lava erupted after the flank collapse are slightly more mafic (56–61 wt% SiO2) and more porphyritic than the ones erupted during the first eruptive phase (58.5–63.5 wt% SiO2). Additionally, patterns of rare earth elements normalized to chondrites show that phase 2 lava are less enriched in LREE than phase 1, and therefore phase 2 lavas may result from slightly higher degrees of partial melting (Germa et al., 2011b). Pre - collapse samples of Piton du Carbet complex (06MT36 and 06MT06) have plagioclase compositions systematically more evolved (An75 to An46) than the post - collapse lavas (Alma, 07MT121, 06MT37) with anorthite compositions as high as An95 (Fig. 5a). Temperatures and water content calculated from plagioclase also show that post - collapse lavas are more volatile - rich and contain crystals that equilibrated at higher temperatures (Fig. 5b, c). Furthermore, biotite and amphibole crystals make some of the largest phenocrysts in the second phase lavas, although biotite was absent in the first phase. Crystal growth might have been enhanced by amphibole dehydration due to rapid magma ascent and decompression rates (Beard et al., 2004; Underwood et al., 2012). Also, plagioclase textures in post - collapse lavas exhibit a larger proportion of sieved crystals, consistent with rapid decompression. Finally, pressures of pyroxene - liquid equilibrium show that post - collapse lavas contain crystals that equilibrated at larger depths (>20 km) than the first phase, suggesting a contribution from deeper magmas not seen in phase 1 samples (Fig. 6b). This disparity between pre - and post - collapse samples of the Piton du Carbet complex suggest a dynamic remobilization of various storage regions immediately after the catastrophic event (Germa et al., 2011), effect that is being discussed in the next section.

5.2.4. Mt. Conil and Mt. Pelée

Samples from the 1902 and 1929–1932 domes of Mt. Pelée yield pyroxene temperatures of −950-1002 °C and pressures up to 1.55 kbar (< 6 km; Fig. 6d). Similarly, plagioclase thermometry and water content (1044–1180 °C and < 1.4 wt% H_2O, Fig. 5) is within range of previously calculated crystallization storage conditions for the basaltic and basaltic-andesite end-members (Gourgaud et al., 1989; Pichavant et al., 2002). Our calculated temperatures and water content represent the magma conditions at crystallization initiation. However, pre-eruptive storage conditions for andesitic and dacitic magmas are systematically lower than 970 °C (Martel et al., 1998; Pichavant et al., 2002). Also, our petrological and chemical results agree to those in previous studies (Pichavant et al., 2002), with plagioclase texture types 1 to 5 and An compositions from $An_{90–48}$ with most chemical trends indicating a normal or oscillatory zonation from core to rim (Supp. Mat 3). Recent eruptions were fed from two distinct magma chambers, one of andesitic to dacitic above 2 kbar (6 km) and another deeper basaltic to basaltic - andesite magmas stored at 7–12 km and 840–900 °C in a vertically elongated and zoned reservoir (Annen et al., 2008; Boudon and Balcone-Boissard, 2021; Gourgaud et al., 1989; Martel et al., 1998; Pichavant et al., 2002). Basaltic magmas intruding shallow reservoirs and triggering eruptions have temperatures of about 1050 °C (Bourdier et al., 1985; Martel et al., 1998; Pichavant et al., 2002).

For the first time, we constrain the crystallization conditions for the early stages of the Mt. Conil - Mt. Pelée complex. The oldest sample from Mt. Conil (06MT28) displays storage in the lower crust, deeper and hotter than the Mt. Pelée magmas. The restricted anorthite composition suggests homogeneous magma sources, although multiple remobilization events are suggested by the presence of all five plagioclase textures. Post-collapse samples, especially Piton Marcel lava dome (09MT130) show that plagioclase crystals formed in the upper crust (<5 km) and were frequently remobilized by the injection of less evolved magma entering the system, as observed by the presence of sieved textures and

resorbed cores (Fig. 4). The sieved textures and restricted temperatures suggest a rapid decompression event was likely initiated by the flank collapse (Fig. 7b). Although the post-collapse lava dome is not significantly more mafic than the rest of Mt. Conil lavas (Germa et al., 2011b), plagioclase compositions are less evolved ($An_{50–85}$) and the magma more volatile - rich (3.5–6.5 wt% H_2O) than for those of the pre - collapse sample (06MT28, $An_{40–55}$, 2–3 wt% H_2O). This drastic change after the collapse suggests a process similar to the one the affected Pitons du Carbet complex in which decompression induced by the deloading at the surface may affect the plumbing system and allows hydrous mafic magmas to ascend from deeper storage, remobilizing the crystal cargo.

5.3. Magmatic evolution following major structural changes

The most direct effect of flank collapse on the plumbing system of a volcano is the decompression of the storage regions as deep as the mantle due to sudden surface unloading leading to variation in magma production rates (Boulesteix et al., 2012; Pinel and Jaupart, 2005; Presley et al., 1997). Many studies investigated the causal links between these large - scale morphological changes at the surface of volcanic edifices and the evolution of magma storage, magma composition, and partial melting (Cornu et al., 2021; Delcamp et al., 2012; Hildenbrand et al., 2004; Hora et al., 2007; Manconi et al., 2009). These studies indicate that flank collapse events are often followed by rapid constructional phases, with higher volume fluxes, changes in eruption dynamics, and changes toward more mafic lava compositions. Comparison of pre- and post- collapse lava compositions show that pre-collapse edifice growth promotes eruption of SiO_2-rich lavas and filters mafic magma (Borgia et al., 2000; Pinel and Jaupart, 2000), whereas post-collapse events are generally more mafic. Similarly, collapse-induced decompression enhances volatile exsolution and decreases magma bulk density, facilitating ascent and eruption of more primitive and crystal - rich magmas (Manconi et al., 2009). The collapse of a volcano's flank consistently results in a reduction of pressure within the underlying storage regions (Pinel and Jaupart, 2000). The influence of a sector collapse on a magmatic reservoir, specifically the extent and rate of decompression, is influenced by the size of the collapsed area, the density of the material, as well as the initial edifice's radius, and the effects diminish with depth (Pinel and Jaupart, 2005; Albino et al., 2010; Pinel and Albino, 2013). For instance, a flank collapse that removed about 700 m of vertical mass at Soufriere Hills Volcano 130 kyr ago, assuming a conical geometry with a radius of approximately 2.5 km, produced a vertical stress reduction of 0.6 MPa and a pressure reduction of 0.18 MPa at 10 km depth (Cassidy et al., 2015).

The sudden reduction in mass can impact the buildup of reservoir pressure and conditions for failure in the magma plumbing system, leading to dike intrusions and substantial changes in its chemical evolution (Pinel and Jaupart, 2005; Manconi et al., 2009; Pinel and Albino, 2013). When the shallower reservoirs are interconnected with deeper magma sources, the reduction in pressure is anticipated to trigger a relatively rapid replenishment of the shallow reservoirs by deeper mafic magmas (Acocella, 2021). Furthermore, decompression of basaltic magmas oversaturated with volatile components at depth is likely to intensify bubble growth and nucleation, and inherently facilitate magma ascent. Consequently, the modifications induced by a sector collapse might introduce additional heat to the system or trigger volatile exsolution in the shallow magma plumbing system, potentially leading to changes in magma composition, viscosity, and enhance explosivity (Acocella, 2021; Romero et al., 2023). All these processes combined enhance the likelihood of eruptions involving denser, more primitive, and crystal-rich magmas as observed in the Lesser Antilles, especially at Mt. Pelée and the Pitons du Carbet complex (Boudon et al., 2007). Most studies investigating the effect of flank collapses on subsequent magma compositions and eruptive styles were focused on intraplate basaltic oceanic islands. A similar series of processes is also observed at silicic island arc volcanoes, and our study shows that it has also been common on Martinique. Flank collapse events have been largely documented for Martinique and other Lesser Antilles islands (Bezard et al., 2017; Boudon et al., 2013; Boudon et al., 2007; Brunet et al., 2016; Harford et al., 2002; Le Friant et al., 2003b; Mattioli et al., 1995; Samper et al., 2008; Cassidy et al., 2015), and all events were followed by rejuvenation of basaltic volcanism. In Martinique, flank collapses that affected Mt. Conil - Mt. Pelée and Pitons du Carbet complexes were followed by eruptions of magmas more mafic than prior to the collapse that progressively evolved again toward andesitic compositions with time (Boudon and Balcone-Boissard, 2021; Germa et al., 2011b; Le Friant et al., 2003b; Boudon et al., 2007). Post-collapse samples systematically show more calcic plagioclase compositions, slightly higher magma temperatures, and more hydrous magmas (Fig. 5). The plagioclase also shows an increase in sieved textures as well as resorbed cores (Fig. 4), indicating faster ascent rates and mixing with a warmer magma. Finally, specifically for Pitons du Carbet complex, post-collapse eruptions are fed by deeper magmas (lower crust) than the pre-collapse ones (upper crust exclusively).

To test our hypothesis that flank collapse can affect plumbing systems within the entire crust, we follow the method of Pinel and Albino (2013) to calculate the effect surface deloading would have on vertical stress and pressure. The large flank collapse of Pitons du Carbet, estimated to have moved $>30\ km^3$ of material down the slopes of the edifice and offshore about 335 ka ago (Boudon et al., 2007; Germa et al., 2011) may have triggered sudden decompression of the plumbing system through the entire crust. We consider the removal of a conical geometry with a height of 800 m and a radius of 4.5 km, with a density of 2400 kg. m^{-3} for dacites of Pitons du Carbet, according to edifice reconstructions (Germa, 2009). We calculate a reduction of the vertical stress by 4.8 MPa and a reduction in pressure of 1.6 MPa at 5 km depth (Fig. 8). These values decrease to 0.5 and 0.1 MPa at 20 km depth (Fig. 8). We can apply the same calculations to the two flank collapses of Mt. Pelée, 126 ka and 36 ka ago, that remobilized 14 and 8 km^3 of material, respectively (Boudon et al., 2007; Germa et al., 2011; Boudon and Balcone-Boissard, 2021). Considering a density of 2500 kg/m^3, a conical geometry with a radius of 2.5 km, and a removed height of 400 m for the first collapse (Germa et al., 2015), we calculate a change in vertical stress and pressure of 1.77 MPa and 0.55 MPa at 5 km depth (Fig. 8). These values decrease to 0.15 MPa and 0.04 MPa at the base of the crust. The 36 ka collapse was much smaller, with a cone radius of 1.5 km and height of 300 m (Germa et al., 2015). Therefore, we obtain vertical stress and pressure changes of 0.35 MPa and 0.10 MPa at 5 km depth, and the changes are negligible at depths larger than 20 km (Fig. 8). Our calculations support the hypothesis that large flank collapses can remobilize silicic systems at mid- to deep- crustal levels at island arcs similarly to basaltic systems at oceanic islands (Manconi et al., 2009). Additionally, as suggested by Cassidy et al. (2015), such calculated pressure variations far exceed the critical overpressure for dyke formation. The decompression magnitudes we calculated in the upper to lower crust beneath Pitons du Carbet might be sufficient to empty shallow silicic reservoirs, initiate dike intrusions, and enhance ascent of basaltic magma from depth.

In summary, collapse events may allow to remobilize mafic magma batches stored at large depths and are likely to initiate magma mixing in shallow reservoirs. This noteworthy eruption-triggering mechanism may lead to the incorporation of distinct crystal populations (Carrara et al., 2019; Bergantz et al., 2015; Jerram and Martin, 2008; Perugini, 2021; Clynne, 1999; Feeley and Dungan, 2002) and subsequently contribute to heightened rates of eruption (Boudon et al., 2007). Additionally, the rate of decompression associated with a flank collapse may result in ascent rates larger than those usually related to reservoir overpressure under normal conditions. Martel et al. (1998), Martel, 2012) have suggested that fast ascent rates from reservoir to fragmentation levels may allow the ascending magma to incorporate other magma batches at various depths in the plumbing system and ascend in a few hours to a few days. This could result in highly explosive Plinian

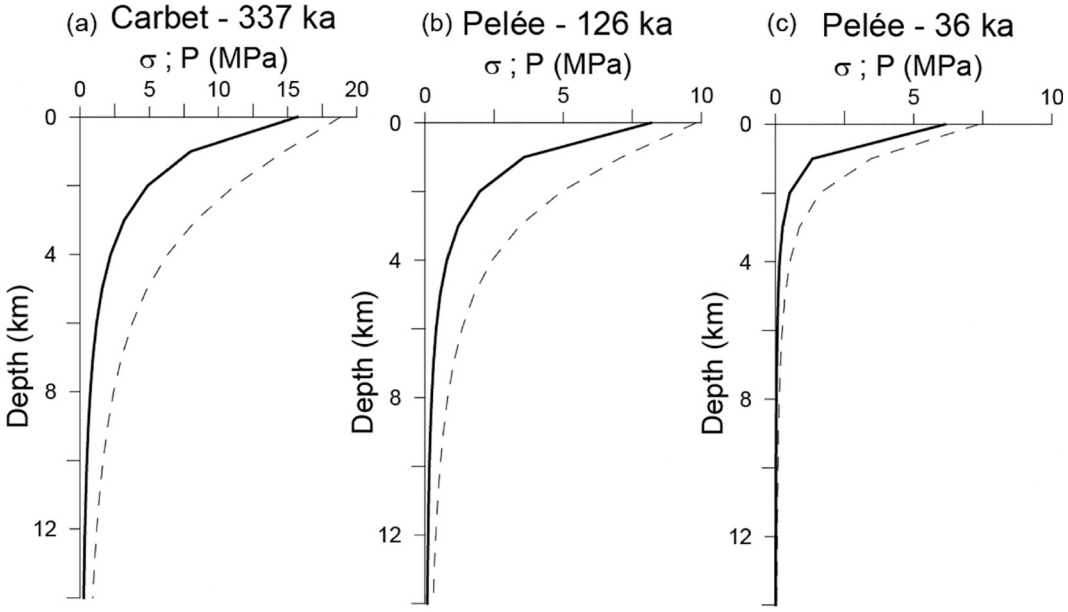

Fig. 8. Vertical stress and pressure reduction under the center of a conical load which is removed from the surface, using Pinel and Albino (2013) equations. Calculations are for an elastic half-space with Poisson's ratio equal to 0.25. The dashed lines are for the vertical component of the stress tensor, s, the bold lines are for the pressure reduction, P, both expressed in MPa. See Supp. Mat. 4 for calculation details. (a) For Pitons du Carbet, we consider a radius of 4.5 km, a height of 800 m, and a density of 2400 kg.m^{-3}. (b) For the 126 ka collapse of Mt. Pelée, we consider a radius a 3.5 km, a height of 400 m, and a density of 2500 kg.m^{-3}. (c) For the 36 ka collapse of Mt. Pelée, we consider a radius of 1.6 km, a height of 300 m, and a density of 2500 kg. m^{-3}.

eruptions, contrasting with Pelean dome-forming eruptions associated with small-volume pyroclastic density currents (Martel, 2012). Such a large deloading magnitude may have promoted the ascent of large volumes of magmas leading to the emplacement of the seven recent lava domes of Pitons du Carbet, that all yield a similar age of 337 ± 3 ka (Germa et al., 2011; Samper et al., 2008).

6. Conclusions

For the first time, we constrain the magma storage conditions at crystallization initiation for the four most recent (<5 Ma) volcanic complexes on Martinique Island. Basaltic magmas are injected into the lower crust and pond at 24–32 km depths, where they evolve by fractional crystallization. Magmas ascend with minimum storage in the middle crust, and storage preferentially develops in the upper crust where they further evolve toward andesitic and dacitic compositions. Shallow mush lenses are frequently remobilized by the injection of mafic magmas that originate in the lower crust. Those frequent injections trigger eruptions. Therefore, recent erupted products often exhibit disequilibrium mineral assemblages, with large variation in compositional signatures and crystal textures.

The south-western Trois Îlets volcanic field displays spatially distributed eruptive vents that are fed by distinct magma batches that do not interact at depth. The magma pathways and temporal distribution are too widespread to allow magma to focus on a central-vent, unlike the northern edifices.

Our study shows that flank collapse events, by displacing edifice's load from the surface offshore, can induce decompression of the plumbing system. The magnitude of the decompression is proportional to the height and radius of the mass removed. The smallest event in Martinique (8 km3) was large enough to affect magma reservoirs down to 4 km depth, while the largest event (30 km3) had the potential to induce decompression as deep as 10–12 km. Such a process promoted the ascent of deep mafic magmas from the lower crust to the surface at relatively fast rates, allowing to remobilize crystals from shallower magma reservoirs. The magma mixing process that resulted from this triggered explosive eruptions allowed a large volume of magma to erupt.

In conclusion, the identified magma storage conditions, and plumbing system architecture for the recent volcanic activity on Martinique island closely resemble those observed in other volcanoes within the Lesser Antilles Island Arc (LAIA), such as Soufriere Hills Volcano, La Soufriere de Guadeloupe, and Soufriere St. Vincent. These newly established correlations offer valuable insights that can aid in the assessment of potential future volcanic eruptions.

Supplementary data to this article can be found online at https://doi.org/10.1016/j.jvolgeores.2023.107972.

Funding

Abigail Martens received funding from the USF Tharp Endowed Scholarship Fund and from the Geological Society of America. Optical microscopy images where acquired with a Keyence VHX - 7000 digital microscope funded by Nation Science Foundation - Instrumentations and facilities to Aurelie Germa and Sylvain Charbonnier (EAR - 2,040,066).

CRediT authorship contribution statement

Abigail Martens: Conceptualization, Data curation, Formal analysis, Funding acquisition, Investigation, Methodology, Visualization, Writing – original draft, Writing – review & editing. **Aurelie Germa:** Conceptualization, Data curation, Formal analysis, Methodology, Supervision, Validation, Visualization, Funding acquisition, Resources, Writing – original draft, Writing – review & editing. **Zachary D. Atlas:** Formal analysis, Supervision, Writing – original draft, Writing – review & editing. **Sylvain Charbonnier:** Data curation, Supervision, Funding acquisition, Writing – review & editing. **Xavier Quidelleur:** Data curation, Supervision, Writing – review & editing.

Declaration of Competing Interest

The authors declare that they have no known competing financial

interests or personal relationships that could have appeared to influence the work reported in this paper.

Data availability

Data is shared in the supplementary materials.

Acknowledgements

The authors thank Abigail Metcalfe and an anonymous reviewer, as well as the editor Ed Llewellin for their thorough review of our manuscript and constructive comments. The authors acknowledge the assistance from Thomas Beasley with EPMA analyses at the Florida Center for Analytical Electron Microscopy at Florida International University. All data associated with this study can be found in the Supplementary Material.

References

Acocella, V., 2021. Volcano flank instability and collapse. In: Volcano-Tectonic Processes. Advances in Volcanology. Springer, Cham. https://doi.org/10.1007/978-3-030-65968-4_6.

Allen, R.W., Collier, J.S., Stewart, A.G., Henstock, T., Goes, S., Rietbrock, A., the VoiLA Team, 2019. The role of arc migration in the development of the Lesser Antilles: A new tectonic model for the Cenozoic evolution of the eastern Caribbean. Geology 47, 891–895. doi:https://doi.org/10.1130/G46708.1.

Albino, F., Pinel, V., Sigmundsson, F., 2010. Influence of surface load variations on eruption likelihood: Application to two Icelandic subglacial volcanoes, Grimsvotn and Katla. Geophys. J. Int. 181, 1510–1524. https://doi.org/10.1111/j.1365-246X.2010.04603.x.

Andreieff, P., Baubron, J.C., Westercamp, D., 1988. Histoire géologique de la Martinique (Petites Antilles): biostratigraphie (foraminifères), radiochronologie (potassium argon), évolution volcano - structurale. Géol. Fr. 39–70.

Annen, C., Pichavant, M., Bachmann, O., Burgisser, A., 2008. Conditions for the growth of a long - lived shallow crustal magma chamber below Mount Pelée volcano (Martinique, Lesser Antilles Arc). J. Geophys. Res. 113, B07209. https://doi.org/10.1029/2007JB005049.

Atlas, Z., Germa, A., Boss, B., Meireles, O., Ward, A., Ryan, J., 2022. Variable element enrichment sources and contributions to volcanic rocks along the Lesser Antilles Island Arc. Front. Earth Sci. 10 https://doi.org/10.3389/feart.2022.782179.

Bachmann, O., Bergantz, G., 2008. The Magma Reservoirs that Feed Supereruptions. Elements 4, 17–21. https://doi.org/10.2113/GSELEMENTS.4.1.17.

Balcone-Boissard, H., Boudon, G., Blundy, J.D., Martel, C., Brooker, R.A., Deloule, E., Solaro, C., Matjuschkin, V., 2018. Deep pre - eruptive storage of silicic magmas feeding Plinian and dome - forming eruptions of central and northern Dominica (Lesser Antilles) inferred from volatile contents of melt inclusions. Contrib. Mineral. Petrol. 173, 101. https://doi.org/10.1007/s00410-018-1528-4.

Balcone-Boissard, H., Boudon, G., d'Augustin, T., Erdmann, S., Deloule, E., Vicente, J., 2023. Architecture of the Lesser Antilles Arc Illustrated by Melt Inclusions. J. Petrol. 64, 6. https://doi.org/10.1093/petrology/egad020.

Barclay, J., Carroll, M.R., Rutherford, M.J., Murphy, M.D., Devine, J.D., Gardner, J., Sparks, R.S.J., 1998. Experimental phase equilibria: constraints on pre-eruptive storage conditions of the Soufriere Hills magma. Geophys. Res. Lett. 25, 3437–3440.

Bardintzeff, J.-M., 1984. Les pyroxénes et leurs inclusions, marqueurs privilégiés des nuees ardentes (Saint-Vincent, Antilles, 1979). Bull. Mineral. 107, 41–54. https://doi.org/10.3406/bulmi.1984.7792.

Bardintzeff, J.M., 1992. Magma mixing processes in volcanic contexts, a thermodynamic approach with the examples of St Vincent Soufrière volcano, West Indies and Cerro Chiquito, Guatemala. Terra Nova 4, 553–556. https://doi.org/10.1111/j.1365 - 3121.1992.tb00597.x.

Beard, J.S., Ragland, P.C., Rushmer, T., 2004. Hydration crystallization reactions between anhydrous minerals and hydrous melt to yield amphibole and biotite in igneous rocks: description and implications. The Journal of Geology 112, 617–621.

Bennett, E.N., Lissenberg, C.J., Cashman, K.V., 2019. The significance of plagioclase textures in mid-ocean ridge basalt (Gakkel Ridge, Arctic Ocean). Contrib Mineral Petrol 174, 49. https://doi.org/10.1007/s00410-019-1587-1.

Bergantz, G., Schleicher, J., Burgisser, A., 2015. Open-system dynamics and mixing in magma mushes. Nat. Geosci. 8, 793–796. https://doi.org/10.1038/ngeo2534.

Bezard, R., Turner, S., Davidson, J., Schmitt, A.K., Lindsay, J., 2017. Origin and Evolution of Silicic Magmas in Oceanic Arcs; an in situ Study from St Lucia, Lesser Antilles. J. Petrol. 58, 1279–1318. https://doi.org/10.1093/petrology/egx053.

Borgia, A., Delaney, P.T., Denlinger, R.P., 2000. Spreading Volcanoes. Borgia Delaney P T Denlinger R P 2000 Spreading VolcanoesAnnual Rev. Earth Planet. Sci. 28, 539–570.

Boudon, G., Balcone-Boissard, H., 2021. Volcanological evolution of Montagne Pelée (Martinique): A textbook case of alternating Plinian and dome - forming eruptions. Earth Sci. Rev. 221, 103754 https://doi.org/10.1016/j.earscirev.2021.103754.

Boudon, G., Le Friant, A., Villemant, B., Viode, J.-P., 2005. Martinique. In: Lindsay, J.M., Robertson, R.E.A., Shepherd, J.B., Ali, S. (Eds.), Volcanic Hazard Atlas of the Lesser Antilles, Trinidad and Tobago, Seismic Res Unit. Univ West Indies, pp. 127–146.

Boudon, G., Le Friant, A., Komorowski, J.-C., Deplus, C., Semet, M.P., 2007. Volcano flank instability in the Lesser Antilles Arc: Diversity of scale, processes, and temporal recurrence. J. Geophys. Res. 112, B08205. https://doi.org/10.1029/2006JB004674.

Boudon, G., Villemant, B., Friant, A.L., Paterne, M., Cortijo, E., 2013. Role of large flank - collapse events on magma evolution of volcanoes. Insights from the Lesser Antilles Arc. J. Volcanol. Geotherm. Res. 263, 224–237. https://doi.org/10.1016/j.jvolgeores.2013.03.009.

Boudon, G., Balcone-Boissard, H., Solaro, C., Martel, C., 2017. Revised chronostratigraphy of recurrent ignimbritic eruptions in Dominica (Lesser Antilles arc): Implications on the behavior of the magma plumbing system. J. Volcanol. Geotherm. Res. 343, 135–154. https://doi.org/10.1016/j.jvolgeores.2017.06.022.

Boulesteix, T., Hildenbrand, A., Gillot, P.Y., Soler, V., 2012. Eruptive response of oceanic islands to giant landslides: New insights from the geomorphologic evolution of the Teide-Pico Viejo volcanic complex (Tenerife, Canary). Geomorphology 138, 6173. https://doi.org/10.1016/j.geomorph.2011.08.025.

Bourdier, J.L., Gourgaud, A., Vincent, P.M., 1985. Magma mixing in a main stage of formation of Montagne Pelée: the Saint Vincent - type scoria flow sequence (Martinique, F.W.I.). J. Volcanol. Geotherm. Res. 25, 309–332. https://doi.org/10.1016/0377 - 0273(85)90019 - 8.

Bouvier, A.S., Métrich, N., Deloule, E., 2008. Slab-Derived Fluids in the Magma sources of St. Vincent (Lesser Antilles Arc): Volatile and Light Element Imprints. J. Petrol. 49, 8, 1427–1448. https://doi.org/10.1093/petrology/egn031.

Bouvier, A.S., Deloule, E., Métrich, N., 2010. Fluid Inputs to Magma sources of St. Vincent and Grenada (Lesser Antilles): New Insights from Trace elements in Olivine-hosted Melt Inclusions. J. Petrol. 51 https://doi.org/10.1093/petrology/egq031, 8,1597–1615.

Bouysse, P., Guennoc, P., 1983. Donnees sur la structure de l'arc insulaire des Petites Antilles, entre Ste - Lucie et Anguilla. Mar. Geol. 53, 131–166. https://doi.org/10.1016/0025 - 3227(83)90038 - 5.

Bouysse, P., Westercamp, D., Andreieff, P., Baubron, J.C., Scolari, G., 1985. Le volcanisme sous - marin Neogenerecent au large des cotesCaraibes des Antilles francaises. In: Relations avec le volcanisme a terre et evolution du front volcanique, pp. 101–114.

Bouysse, P., Westercamp, D., Andreieff, P., 1990. The Lesser Antilles Island Arc. In: Proceedings of the Ocean Drilling Program. Ocean Drilling Program. https://doi.org/10.2973/odp.proc.sr.110.1990.

Briden, J.C., Rex, D.C., Faller, A.M., Tomblin, J.F., 1979. K - Ar Geochronology and Palaeomagnetism of Volcanic Rocks in the Lesser Antilles Island Arc. Philos. Trans. R. Soc. Lond. Ser. Math. Phys. Sci. 291, 485–528.

Brunet, M., Le Friant, A., Boudon, G., Lafuerza, S., Talling, P., Hornbach, M., Ishizuka, O., Lebas, E., Guyard, H., IODP Expedition 340 Science Party, 2016. Composition, geometry, and emplacement dynamics of a large volcanic island landslide offshore Martinique: from volcano flank - collapse to seafloor sediment failure?: SUBMARINE LANDSLIDES OFFSHORE MARTINIQUE. Geochem. Geophys. Geosyst. 17, 699–724. https://doi.org/10.1002/2015GC006034.

Burchardt, S., Galland, O., 2016. Studying Volcanic Plumbing Systems – Multidisciplinary Approaches to a Multifaceted Problem. In: Nemeth, K. (Ed.), Updates in Volcanology - from Volcano Modelling to Volcano Geology. InTech. https://doi.org/10.5772/63959.

Camejo-Harry, M., Melekhova, E., Blundy, J., Attridge, W., Robertson, R., Christopher, T., 2018. Magma evolution beneath Bequia, Lesser Antilles, deduced from petrology of lavas and plutonic xenoliths. Contrib. Mineral. Petrol. 173, 77. https://doi.org/10.1007/s00410 - 018 - 1504 - z.

Camejo-Harry, M., Melekhova, E., Blundy, J., Robertson, R., 2019. Evolution in magma storage conditions beneath Kick - 'em - Jenny and Kick - 'em - Jack submarine volcanoes, Lesser Antilles arc. J. Volcanol. Geotherm. Res. 373, 1–22. https://doi.org/10.1016/j.jvolgeores.2019.01.023.

Carrara, A., Burgisser, A., Bergantz, G.W., 2019. Lubrication effects on magmatic mush dynamics, 2019. J. Volcanol. Geotherm. Res. 380 https://doi.org/10.1016/j.jvolgeores.2019.05.008.

Cashman, K.V., Sparks, R.S.J., Blundy, J.D., 2017. Vertically extensive and unstable magmatic systems: A unified view of igneous processes. Science 355, eaag3055. https://doi.org/10.1126/science.aag3055.

Cassidy, M., Watt, S.F.L., Talling, P.J., Palmer, M.R., Edmonds, M., Jutzeler, M., Wall-Palmer, D., Manga, M., Coussens, M., Gernon, T., Taylor, R.N., Michalik, A., Inglis, E., Breitkreus, C., Le Friant, A., Ishizuka, O., Boudon, G., McCanta, M.C., Adachi, T., Hornbach, M.J., Colas, S.L., Endo, D., Fujjinawa, A., Kataoka, K.S., Maeno, F., Tamura, Y., Wang, F., 2015. Rapid onset of mafic magmatism facilitated by volcanic edifice collapse. Geophys. Res. Lett. 42, 4778–4785. https://doi.org/10.1002/2015GL064519.

Christeson, G.L., Bangs, N.L., Shipley, T.H., 2003. Deep structure of an island arc backstop, Lesser Antilles subduction zone: lesser antilles backstop structure. J. Geophys. Res. Solid Earth 108. https://doi.org/10.1029/2002JB002243.

Christopher, T., Edmonds, M., Taisne, B., Odbert, H., Costa, A., Hards, V., Wadge, G., 2015. Periodic Sulphur dioxide degassing from the Soufrière Hills Volcano related to deep magma supply. Geol. Soc. Lond. Spec. Publ. 410, 123–141. https://doi.org/10.1144/SP410.11.

Cooper, K.M., Kent, A.J.R., 2014. Rapid remobilization of magmatic crystals kept in cold storage. Nature 506, 480–483. https://doi.org/10.1038/nature12991.

Cooper, G.F., Davidson, J.P., Blundy, J.D., 2016. Plutonic xenoliths from Martinique, Lesser Antilles: evidence for open system processes and reactive melt flow in island arc crust. Contrib. Mineral. Petrol. 171, 87. https://doi.org/10.1007/s00410 - 016 - 1299 - 8.

Clynne, M.A., 1999. A complex magma mixing origin for rocks erupted in 1915, Lassen Peak, California. J Petrol 40 (1), 105–132.

Cooper, G.F., Blundy, J.D., Macpherson, C.G., Humphreys, M.C.S., Davidson, J.P., 2019. Evidence from plutonic xenoliths for magma differentiation, mixing and storage in a volatile - rich crystal mush beneath St. Eustatius, Lesser Antilles. Contrib. Mineral. Petrol. 174, 39. https://doi.org/10.1007/s00410 - 019 - 1576 - 4.

Cooper, G.F., Macpherson, C.G., Blundy, J.D., et al., 2020. Variable water input controls evolution of the Lesser Antilles volcanic arc. Nature 582, 525–529. https://doi.org/10.1038/s41586-020-2407-5.

Cornu, M.-N., Paris, R., Doucelance, R., Bachélery, P., Bosq, C., Auclair, D., Benbakkar, M., Gannoun, A.M., Guillou, H., 2021. Exploring the links between volcano flank collapse and the magmatic evolution of an ocean island volcano: Fogo, Cape Verde. Sci. Rep. 11, 17478. https://doi.org/10.1038/s41598-021-96897-1.

Coulon, C., Clocchiatti, R., Maury, R.C., Westercamp, D., 1984. Petrology of basaltic xenoliths in andesitic to dacitic host lavas from Martinique (lesser antilles): evidence for magma mixing. Bull. Volcanol. 47, 705–734. https://doi.org/10.1007/BF01952340.

d'Arco, Ph., Maury, R.C., Westercamp, D., 1981. Geothermometry and geobarometry of a cummingtonite - bearing dacite from Martinique, Lesser Antilles. Contrib. Mineral. Petrol. 77, 177–184. https://doi.org/10.1007/BF00636521.

d'Augustin, T., Balcone-Boissard, H., Boudon, G., Martel, C., Deloule, E., Bürckel, P., 2020. Evidence for an active, Transcrustal Magma System in the last 60 ka and Eruptive Degassing Budget (H_2O, CO_2, S, F, Cl, Br): the Case of Dominica. Geochem. Geophys. Geosyst. 21 https://doi.org/10.1029/2020GC009050.

Delcamp, A., van Wyk de Vries, B., James, M.R., Gailler, L.S., Lebas, E., 2012. Relationships between volcano gravitational spreading and magma intrusion. Bull. Volcanol. 74, 743–765. https://doi.org/10.1007/s00445 - 011 - 0558 - 9.

Deng, F., Connor, C.B., Malservisi, R., Connor, L.J., White, J.T., Germa, A., Wetmore, P. H., 2017. A geophysical model for the origin of volcano vent clusters in a colorado plateau volcanic field: origin of volcano clusters. J. Geophys. Res. Solid Earth 122, 8910–8924. https://doi.org/10.1002/2017JB014434.

Devine, J.D., Rutherford, M.J., Gardner, J.E., 1998. Petrologic determination of ascent rates for the 1995–1997 Soufriere Hills Volcano andesitic magma. Geophys. Res. Lett. 25, 3673–3676. https://doi.org/10.1029/98GL00912.

Druitt, T.H., Young, S.R., Baptie, B., Bonadonna, C., Calder, E.S., Clarke, A.B., Cole, P.D., Harford, C.L., Herd, R.A., Luckett, R., Ryan, G., Voight, B., 2002. Episodes of cyclic Vulcanian explosive activity with fountain collapse at Soufrière Hills Volcano. Montserrat. Geol. Soc. Lond. Mem. 21, 281–306. https://doi.org/10.1144/GSL.MEM.2002.021.01.13.

Edmonds, M., Kohn, S.C., Hauri, E.H., Humphreys, M.C.S., Cassidy, M., 2016. Extensive, water - rich magma reservoir beneath southern Montserrat. Lithos 252–253, 216–233. https://doi.org/10.1016/j.lithos.2016.02.026.

Feeley, T.C., Dungan, M.A., 2002. Mafic-felsic magma interaction at Satsuma-Iwojima volcano, Japan: evidence from mafic inclusions in rhyolites. Earth Planet Sp. 54, 303–325. https://doi.org/10.1186/BF03353030.

Fichaut, M., Maury, R.C., Traineau, H., Westercamp, D., Joron, J.L., Gourgaud, A., Coulon, C., 1989. Magmatology of Mt. Pelée (Martinique, F.W.I.). III: Fractional crystallization versus magma mixing. J. Volcanol. Geotherm. Res. 38, 189–213. https://doi.org/10.1016/0377 - 0273(89)90037 - 1.

Fontaine, F.R., Komorowski, J.-C., Corbeau, J., Burtin, A., Jadelus, F., Melezan, D., Vidal, C., Zimmermann, B., Lavenaire, J.-M., Gabriel, J.-G., Saurel, J.-M., Lemarchand, A., Grandin, R., de Chabalier, J.-B., Beauducel, F., Moune, S., Chilun-Eusebe, E., Robert, V., Moretti, R., Boudon, G., Carazzo, G., Michaud-Dubuy, A., Tait, S., 2021. Report on Pelee (France). Global Volcanism Program, 2021. In: Bennis, K.L., Venzke, E. (Eds.), Bulletin of the Global Volcanism Network, 46:7. Smithsonian Institution. https://doi.org/10.5479/si.GVP.BGVN202107-360120.

Fontaine, F.R., Komorowski, J.-C., Corbeau, J., Burtin, A., Grandin, R., de Saurel Chabalier, J.-B., Beauducel, F., Agrinier, P., Moretti, R., Moune, S.J.-M., Jadelus, F., Melezan, D., Gabriel, J.-G., Vidal, C., Zimmermann, B., Vaton, D., Koziol, J., Lavenaire, J.-M., Filliaert, A., Chilun-Eusebe, E., Inostroza, M., M'etazian, J.-P., Satriano, C., Vall'ee, M., Potier, A., Jessop, D.E., Robert, V., Deroussi, S., Lemarchand, A., Carazzo, G., Bonaim'e, S., Le Friant, A., Chaussion, M., Michaud-Dubuy, A., Tait, S., Retailleau, L., Andrieu, A., di Muro, A., Allard, P., Vlastelic, I., 2022. Volcanic unrest of Mount Pel'ee (Martinique, France). IAVCEI General Assembly, Rotorua, New Zealand, 30 Jan – 4 february 2023.

Gadalia, A., Baltassat, J.M., Bouchot, V., Caritg-Monnot, S., Gal, F., Girard, J.F., Gutierrez, A., Jacob, T., Martelet, G., Coppo, N., Rad, S.H., Taïlamé, A., Traineau, H., Vittecoq, B., Wawrzyniak, P., Zammit, C., 2014. A new insight of the geothermal systems of the Martinique Island (Lesser Antilles): results of the 2012-2013 exploration. Deep Geothermal Days, Apr 2014, Paris, France. ffhal-00945847f. https://hal-brgm.archives-ouvertes.fr/hal-01102469.

Galland, O., Bertelsen, H.S., Eide, C.H., Guldstrand, F., Haug, Ø.T., Leanza, H.A., Mair, K., Palma, O., Planke, S., Rabbel, O., Rogers, B., Schmiedel, T., Souche, A., Spacapan, J.B., 2018. Storage and Transport of Magma in the Layered Crust—formation of sills and related flat - lying intrusions. In: Volcanic and Igneous Plumbing Systems. Elsevier, pp. 113–138. https://doi.org/10.1016/B978 - 0 - 12 - 809749 - 6.00005 - 4.

Garmon, W.T., Allen, C.D., Groom, K.M., 2017. Geologic and Tectonic Background of the Lesser Antilles. In: Allen, C.D. (Ed.), Landscapes and Landforms of the Lesser Antilles. World Geomorphological Landscapes. Springer International Publishing, Cham, pp. 7–15. https://doi.org/10.1007/978-3-319-55787-8_2.

George, O.A., Malservisi, R., Govers, R., Connor, C.B., Connor, L.J., 2016. Is uplift of volcano clusters in the Tohoku Volcanic Arc, Japan, driven by magma accumulation in hot zones? A geodynamic modeling study: magma underplating investigation. J. Geophys. Res. Solid Earth 121, 4780–4796. https://doi.org/10.1002/2016JB012833.

Germa, A., 2009. Evolution volcano-tectonique de l'île de la Martinique (arc insulaire des Petites Antilles): nouvelles contraintes géochronologiques et géomorphologiques. PhD dissertation, Université Paris-Sud, Orsay, France. https://tel.archives-ouvertes.fr/tel-00447342.

Germa, A., Quidelleur, X., Labanieh, S., Chauvel, C., Lahitte, P., 2011a. The volcanic evolution of Martinique Island: Insights from K–Ar dating into the Lesser Antilles arc migration since the Oligocene. J. Volcanol. Geotherm. Res. 208, 122–135. https://doi.org/10.1016/j.jvolgeores.2011.09.007Germa.

Germa, A., Quidelleur, X., Labanieh, S., Lahitte, P., Chauvel, C., 2010. The eruptive history of Morne Jacob volcano (Martinique Island, French West Indies): Geochronology, geomorphology and geochemistry of the earliest volcanism in the recent Lesser Antilles arc. J. Volcanol. Geother. Res. 198 (3–4), 297–310. https://doi.org/10.1016/j.jvolgeores.2010.09.013.

Germa, A., Quidelleur, X., Lahitte, P., Labanieh, S., Chauvel, C., 2011b. The K–ArCassignol–Gillot technique applied to western Martinique lavas: A record of Lesser Antilles arc activity from 2Ma to Mount Pelée volcanism. Quat. Geochronol. 6, 341–355. https://doi.org/10.1016/j.quageo.2011.02.001.

Germa, A., P. Lahitte, and X. Quidelleur. 2015. Construction and destruction of Mont Pelée volcano: Volumes and rates constrained from a geomorphological model of evolution, J. Geophys. Res. Earth Surf., 120, 1206–1226, doi:10.1002/2014JF003355.

Gourgaud, A., Fichaut, M., Joron, J.-L., 1989. Magmatology of Mt. Pelde (Martinique, F. W.I.). I: Magma mixing and triggering of the 1902 and 1929 Pelean nudes ardentes. J. Volcanol. Geotherm. Res. 38, 143–169.

Gurenko, A.A., Trumbull, R.B., Thomas, R., Lindsay, J.M., 2005. A Melt Inclusion Record of Volatiles, Trace elements and Li–B Isotope Variations in a Single Magma System from the Plat Pays Volcanic complex, Dominica, Lesser Antilles. J. Petrol. 46, 2495–2526. https://doi.org/10.1093/petrology/egi063.

Halama, R., Boudon, G., Villemant, B., Joron, J.-L., Le Friant, A., Komorowski, J.-C., 2006. Pre - eruptive crystallization conditions of mafic and silicic magmas at the Plat Pays volcanic complex, Dominica (Lesser Antilles). J. Volcanol. Geotherm. Res. 153, 200–220. https://doi.org/10.1016/j.jvolgeores.2005.12.001.

Harford, C.L., Pringle, M.S., Sparks, R.S.J., Young, S.R., 2002. The volcanic evolution of Montserrat using $^{40}Ar/^{39}Ar$ geochronology. Geol. Soc. Lond. Mem. 21, 93–113. https://doi.org/10.1144/GSL.MEM.2002.021.01.05.

Heath, E., Macdonald, R., Belkin, H., Hawkesworth, C., Sigurdsson, H., 1998. Magmagenesis at Soufriere Volcano, St Vincent, Lesser Antilles Arc. J. Petrol. 39, 1721–1764. https://doi.org/10.1093/petroj/39.10.1721.

Higgins, O., Caricchi, L., 2023. Eruptive dynamics reflect crustal structure and mantle productivity beneath volcanoes. Geology. https://doi.org/10.1130/G51355.1.

Higgins, O., Sheldrake, T., Caricchi, L., 2021. Quantitative chemical mapping of plagioclase as a tool for the interpretation of volcanic stratigraphy: an example from Saint Kitts. Lesser Antilles. Bull. Volcanol. 83, 51. https://doi.org/10.1007/s00445 - 021 - 01476 - x.

Hildenbrand, A., Gillot, P.-Y., Le Roy, I., 2004. Volcano - tectonic and geochemical evolution of an oceanic intra - plate volcano: Tahiti - Nui (French Polynesia). Earth Planet. Sci. Lett. 217, 349–365. https://doi.org/10.1016/S0012 - 821X(03)00599 - 5.

Hora, J.M., Singer, B.S., Worner, G., 2007. Volcano evolution and eruptive flux on the thick crust of the Andean Central Volcanic Zone: 40Ar/39Ar constraints from Volcan Parinacota. Chile. Geol. Soc. Am. Bull. 119, 343–362. https://doi.org/10.1130/B25954.1.

Jerram, D.A., Martin, V.M., 2008. Understanding crystal populations and their significance through the magma plumbing system. Geol. Soc. Lond. Spec. Publ. 304, 133–148. https://doi.org/10.1144/SP304.7.

Jochum, K.P., Willbold, M., Raczek, I., Stoll, B., Herwig, K., 2005. Chemical Characterisation of the USGS Reference Glasses GSA - 1G, GSC - 1G, GSD - 1G, GSE - 1G, BCR - 2G, BHVO - 2G and BIR - 1G using EPMA, ID - TIMS, ID - ICP - MS and LA - ICP - MS. Geostand. Geoanal. Res. 29, 285–302. https://doi.org/10.1111/j.1751 - 908X.2005.tb00901.x.

Kavanagh, J.L., Menand, T., Sparks, R.S.J., 2006. An experimental investigation of sill formation and propagation in layered elastic media. Earth Planet. Sci. Lett. 245, 799–813. https://doi.org/10.1016/j.epsl.2006.03.025.

Kopp, H., Weinzierl, W., Becel, A., Charvis, P., Evain, M., Flueh, E.R., Gailler, A., Galve, A., Hirn, A., Kandilarov, A., Klaeschen, D., Laigle, M., Papenberg, C., Planert, L., Roux, E., 2011. Deep structure of the Central Lesser Antilles Island Arc: Relevance for the formation of continental crust. Earth Planet. Sci. Lett. 304, 121–134. https://doi.org/10.1016/j.epsl.2011.01.024.

Labanieh, S., Chauvel, C., Germa, A., Quidelleur, X., Lewin, E., 2010. Isotopic hyperbolas constrain sources and processes under the Lesser Antilles arc. Earth Planet. Sci. Lett. 298, 35–46. https://doi.org/10.1016/j.epsl.2010.07.018.

Labanieh, S., Chauvel, C., Germa, A., Quidelleur, X., 2012. Martinique: a Clear Case for Sediment Melting and Slab Dehydration as a Function of Distance to the Trench. J. Petrol. 53, 2441–2464. https://doi.org/10.1093/petrology/egs055.

Lange, R.A., Frey, H.M., Hector, J., 2009. A thermodynamic model for the plagioclase - liquid hygrometer/thermometer. Am. Mineral. 94, 494–506. https://doi.org/10.2138/am.2009.3011.

Le Friant, A., Boudon, G., Deplus, C., Villemant, B., 2003a. Large - scaleflank collapse eventsduring the activity of Montagne Pelée, Martinique, Lesser Antilles: flank collapses on montagne pelée volcano. J. Geophys. Res. Solid Earth 108. https://doi.org/10.1029/2001JB001624.

Le Friant, A., Heinrich, P., Deplus, C., Boudon, G., 2003b. Numerical simulation of THE last flank - collapse event of Montagne Pelée, Martinique, Lesser Antilles: numerical simulation of the last flank - collapse event. Geophys. Res. Lett. 30 https://doi.org/10.1029/2002GL015903.

Legendre, L., Philippon, M., Münch, Ph., Leticée, J.L., Noury, M., Maincent, G., Cornée, J. J., Caravati, A., Lebrun, J.F., Mazabraud, Y., 2018. Trench Bending Initiation: Upper Plate Strain Pattern and Volcanism. Insights from the Lesser Antilles Arc, St.

Barthelemy Island, French West Indies. Tectonics 37, 2777–2797. https://doi.org/10.1029/2017TC004921.
Lindsay, J.M., Trumbull, R.B., Siebel, W., 2005. Geochemistry and petrogenesis of late Pleistocene to recent volcanism in Southern Dominica, Lesser Antilles. J. Volcanol. Geotherm. Res. 148, 253–294. https://doi.org/10.1016/j.jvolgeores.2005.04.018.
Maccaferri, F., Bonafede, M., Rivalta, E., 2010. A numerical model of dyke propagation in layered elastic media. Geophys. J. Int. 180, 1107–1123. https://doi.org/10.1111/j.1365 - 246X.2009.04495.x.
Macdonald, R., Hawkesworth, C.J., Heath, E., 2000. The Lesser Antilles volcanic chain: a study in arc magmatism. Earth Sci. Rev. 49, 1–76. https://doi.org/10.1016/S0012 - 8252(99)00069 - 0.
Manconi, A., Longpre, M.-A., Walter, T.R., Troll, V.R., Hansteen, T.H., 2009. The effects of flank collapses on volcano plumbing systems. Geology 37, 1099–1102. https://doi.org/10.1130/G30104A.1.
Martel, C., 2012. Eruption Dynamics Inferred from Microlite Crystallization experiments: Application to Plinian and Dome - forming Eruptions of Mt. Pelée (Martinique, Lesser Antilles). J. Petrol. 53, 699–725. https://doi.org/10.1093/petrology/egr076.
Martel, C., Pichavant, M., Bourdier, J., Traineau, H., Holtz, F., Scaillet, B., 1998. Magma storage conditions and control of eruption regime in silicic volcanoes: experimental evidence from Mt. Pelée. Earth Planet. Sci. Lett. 156, 89–99. https://doi.org/10.1016/S0012 - 821X(98)00003 - X.
Martel, C., Radadi Ali, A., Poussineau, S., Gourgaud, A., Pichavant, M., 2006. Basalt - inherited microlites in silicic magmas: evidence from Mount Pelée (Martinique, French West Indies). Geology 34, 905. https://doi.org/10.1130/G22672A.1.
Mattioli, G.S., Jansma, P.E., Jaramillo, L., Smith, A.L., 1995. Sector Collapse in Island Arc Volcanoes: a Digital Topographic and Bathymetric Investigation of the Qualibou Depression, St. Lucia, Lesser Antilles. Caribb. J. Sci. 31, 163–173.
Melekhova, E., Blundy, J., Robertson, R., Humphreys, M.C.S., 2015. Experimental evidence for polybaric differentiation of Primitive Arc Basalt beneath St. Vincent, Lesser Antilles. J. Petrol. 56, 161–192. https://doi.org/10.1093/petrology/egu074.
Melekhova, E., Blundy, J., Martin, R., Arculus, R., Pichavant, M., 2017. Petrological and experimental evidence for differentiation of water - rich magmas beneath St. Kitts, Lesser Antilles. Contrib. Mineral. Petrol. 172, 98. https://doi.org/10.1007/s00410-017-1416-3.
Melekhova, E., Schlaphorst, D., Blundy, J., Kendall, J.-M., Connolly, C., McCarthy, A., Arculus, R., 2019. Lateral variation in crustal structure along the Lesser Antilles arc from petrology of crustal xenoliths and seismic receiver functions. Earth Planet. Sci. Lett. 516, 12–24. https://doi.org/10.1016/j.epsl.2019.03.030.
Metcalfe, A., Moune, S., Komorowski, J.-C., Kilgour, G., Jessop, D.E., Moretti, R., Legendre, Y., 2021. Magmatic Processes at La Soufrière de Guadeloupe: Insights from Crystal Studies and Diffusion Timescales for Eruption Onset. Front. Earth Sci. 9, 617294 https://doi.org/10.3389/feart.2021.617294.
Metcalfe, A., Moune, S., Komorowski, J.C., Moretti, R., 2022. 2022, Bottom-up vs top-down drivers of eruption style: Petro-geochemical constraints from the holocene explosive activity at La Soufrière de Guadeloupe. J. Volcanol. Geotherm. Res. 424 https://doi.org/10.1016/j.jvolgeores.2022.107488.
Metcalfe, A., Moune, S., Komorowski, J.C., Robertson, R., Christopher, T.E., Joseph, E.P., Moretti, R., 2023. 2023, Diverse magma storage and major and volatile magma composition: what are the implications on the eruptive style across a volcanic arc? An example of the Lesser Antilles Arc. Earth Sci. Rev. 241 https://doi.org/10.1016/j.earscirev.2023.104440.
Michaud-Dubuy, A., 2019. Dynamique des éruptions pliniennes : réévaluation de l'aléa volcanique en Martinique (Dissertation). Université de Paris, Institut de Physique du Globe de Paris.
Murphy, M.D., Sparks, R.S.J., Barclay, J., Carroll, M.R., Lejeune, A.-M., Brewer, T.S., Macdonald, R., Black, S., Young, S., 1998. The role of magma mixing in triggering the current eruption at the Soufriere Hills volcano, Montserrat, West Indes. Geophys. Res. Lett. 25, 1–4.
Murphy, M.D., Sparks, R.S.J., Barclay, J., Carroll, M.R., Brewer, T.S., 2000. Remobilization of Andesite Magma by Intrusion of Mafic Magma at the Soufriere Hills Volcano, Montserrat, West Indies. J. Petrol. 41, 21–42. https://doi.org/10.1093/petrology/41.1.21.
Murray, R.W., Miller, D.J., Kryc, K.A., 2000. Analysis of major and trace elements in rocks, sediments, and interstitial waters by inductively coupled plasma–atomic emission spectrometry (ICP - AES). ODP Tech Note 29. https://doi.org/10.2973/odp.tn.29.2000.
Nagle, F., Stipp, J.J., Fisher, D.E., 1976. K - Ar geochronology of the Limestone Caribbees and Martinique, Lesser Antilles, West Indies. Earth Planet. Sci. Lett. 29, 401–412. https://doi.org/10.1016/0012 - 821X(76)90145 - X.
Neave, D.A., Putirka, K.D., 2017. A new clinopyroxene - liquid barometer, and implications for magma storage pressures under Icelandic rift zones. Am. Mineral. 102, 777–794. https://doi.org/10.2138/am - 2017 - 5968.
Noury, M., Philippon, M., Cornée, J., Bernet, M., Bruguier, O., Montheil, L., Legendre, L., Dugamin, E., Bonno, M., Münch, P., 2021. Evolution of a Shallow Volcanic Arc Pluton during Arc Migration: A Tectono-thermal Integrated Study of the St. Martin Granodiorites (Northern Lesser Antilles). Geochem. Geophys. Geosyst. 22 https://doi.org/10.1029/2020GC009627.
Ostorero, L., Boudon, G., Balcone-Boissard, H., Morgan, D.J., d'Augustin, T., Solaro, C., 2021. Time - window into the transcrustal plumbing system dynamics of Dominica (Lesser Antilles). Sci. Rep. 11, 11440. https://doi.org/10.1038/s41598 - 021 - 90831 - 1.
Perugini, D., 2021. Magma Mixing: The Trigger for Explosive Volcanic Eruptions. In: The Mixing of Magmas. Advances in Volcanology. Springer, Cham. https://doi.org/10.1007/978-3-030-81811-1_10.
Pichavant, M., Macdonald, R., 2007. Crystallization of primitive basaltic magmas at crustal pressures and genesis of the calc-alkaline igneous suite: experimental evidence from St. Vincent, Lesser Antilles arc. Contrib. Mineral. Petrol. 145, 535–558. https://doi.org/10.1007/s00410-007-0208-6.
Pichavant, M., Martel, C., Bourdier, J.-L., Scalliet, B., 2002. Physical conditions, structure, and dynamics of a zoned magma chamber: Mount Pelée (Martinique, Lesser Antilles Arc). J. Geophys. Res. 107, 2093. https://doi.org/10.1029/2001JB000315.
Pichavant, M., Poussineau, S., Lesne, P., Solaro, C., Bourdier, J.-L., 2018. Experimental Parametrization of Magma Mixing: Application to the ad 1530 Eruption of La Soufrière, Guadeloupe (Lesser Antilles). J. Petrol. 59, 257–282. https://doi.org/10.1093/petrology/egy030.
Pinel, V., Albino, F., 2013. Consequences of volcano sector collapse on magmatic storage zones: insights from numerical modeling. J. Volcanol. Geotherm. Res. 252, 29–37. https://doi.org/10.1016/j.jvolgeores.2012.11.009.
Pinel, V., Jaupart, C., 2000. The effect of edifice load on magma ascent beneath a volcano. Philos. Trans. R. Soc. Lond. Ser. Math. Phys. Eng. Sci. 358, 1515–1532. https://doi.org/10.1098/rsta.2000.0601.
Pinel, V., Jaupart, C., 2005. Some consequences of volcanic edifice destruction for eruption conditions. J. Volcanol. Geotherm. Res. 145, 68–80. https://doi.org/10.1016/j.jvolgeores.2005.01.012.
Presley, T.K., Sinton, J.M., Pringle, M., 1997. Postshield volcanism and catastrophic mass wasting of the Waianae Volcano, Oahu, Hawaii. Bull. Volcanol. 58, 597–616. https://doi.org/10.1007/s004450050165.
Putirka, K.D., 2005. Igneous thermometers and barometers based on plagioclase + liquid equilibria: Tests of some existing models and new calibrations. Am. Mineral. 90, 336–346. https://doi.org/10.2138/am.2005.1449.
Putirka, K.D., 2008. Thermometers and Barometers for Volcanic Systems. Rev. Mineral. Geochem. 69, 61–120. https://doi.org/10.2138/rmg.2008.69.3.
Putirka, K., Condit, C.D., 2003. Cross section of a magma conduit system at the margin of the Colorado Plateau. Geology 31, 701. https://doi.org/10.1130/G19550.1.
Romero, J.E., Polacci, M., Arzilli, F., Schipper C. Ian, La Spina G., Burton M., Parada A., Norambuena J., Guevara A., Watt S., Moreno H., Franco L., Fellowes J. *2023.* Long-term volcano evolution controlled by lateral collapse at Antuco volcano, southern Andes, Chile. *Commun Earth Environ* **4**, 292 . doi: 10.1038/s43247-023-00931-1.
Renjith, M.L., 2014. Micro - textures in plagioclase from 1994–1995 eruption, Barren Island Volcano: evidence of dynamic magma plumbing system in the Andaman subduction zone. Geosci. Front. 5, 113–126. https://doi.org/10.1016/j.gsf.2013.03.006.
Rojas-Agramonte, Y., Williams, I.S., Arculus, R., Kröner, A., García-Casco, A., Lázaro, C., Buhre, S., Wong, J., Geng, H., Echeverría, C.M., Jeffries, T., Xie, H., Mertz-Kraus, R., 2017. Ancient xenocrystic zircon in young volcanic rocks of the southern Lesser Antilles island arc. Lithos 290–291, 228–252. https://doi.org/10.1016/j.lithos.2017.08.002.
Roobol, M.J., Smith, A.L., 1976. Mount Pelée, Martinique: A pattern of alternating eruptive styles. Geology 4, 521. https://doi.org/10.1130/0091 - 7613(1976)4<521:MPMAPO>2.0.CO;2.
Rowley, K., 1978. Late Pleistocene pyroclastic deposits of Soufrière Volcano, St. Vincent, West Indies. Geol. Soc. Am. Bull. 89, 825. https://doi.org/10.1130/0016-7606(1978)89<825:LPPDOS>2.0.CO;2.
Rutherford, M.J., Devine, J.D., 2003. Magmatic conditions and magma ascent as indicated by hornblende phase equilibrium and reactions in the 1995-2002 Soufrière Hills Magma. J. Petrol. 44, 1433–1454.
Samper, A., Quidelleur, X., Boudon, G., Le Friant, A., Komorowski, J.C., 2008. Radiometric dating of three large volume flank collapses in the Lesser Antilles Arc. J. Volcanol. Geotherm. Res. 176, 485–492. https://doi.org/10.1016/j.jvolgeores.2008.04.018.
Samper, A., Quidelleur, X., Komorowski, J.-C., Lahitte, P., Boudon, G., 2009. Effusive history of the Grande Découverte Volcanic Complex, southern Basse - Terre (Guadeloupe, French West Indies) from new K–ArCassignol–Gillot ages. J. Volcanol. Geotherm. Res. 187, 117–130. https://doi.org/10.1016/j.jvolgeores.2009.08.016.
Schlaphorst, D., Melekhova, E., Kendall, J.-M., Blundy, J., Latchman, J.L., 2018. Probing layered arc crust in the Lesser Antilles using receiver functions. R. Soc. Open Sci. 5, 180764 https://doi.org/10.1098/rsos.180764.
Smith, A.L., Roobol, M.J., 1990. Mt. Pelée, Martinique: A Study of an Active Island - Arc Volcano. Geological Society of America.
Solaro, C., Martel, C., Champallier, R., Boudon, G., Balcone-Boissard, H., Pichavant, M., 2019. Petrological and experimental constraints on magma storage for large pumiceous eruptions in Dominica island (Lesser Antilles). Bull. Volcanol. 81, 55. https://doi.org/10.1007/s00445 - 019 - 1313 - x.
Stamper, C.C., Blundy, J.D., Arculus, R.J., Melekhova, E., 2014. Petrology of Plutonic Xenoliths and Volcanic Rocks from Grenada, Lesser Antilles. J. Petrol. 55, 1353–1387. https://doi.org/10.1093/petrology/egu027.
Streck, M.J., 2008. Mineral Textures and Zoning as evidence for Open System Processes. Rev. Mineral. Geochem. 69, 595–622. https://doi.org/10.2138/rmg.2008.69.15.
Taylor, J., 1997. An Introduction to Error Analysis: The Study of Uncertainties in Physical Measurements, Second Edition. University Science books, p. 327pp.
Tollan, P.M.E., Bindeman, I., Blundy, J.D., 2012. Cumulate xenoliths from St. Vincent, Lesser Antilles Island Arc: a window into upper crustal differentiation of mantle - derived basalts. Contrib. Mineral. Petrol. 163, 189–208. https://doi.org/10.1007/s00410 - 011 - 0665 - 9.
Toothill, J., Williams, C.A., MacDonald, R., Turner, S.P., Rogers, N.W., Hawkesworth, C. J., Jerram, D.A., Ottley, C.J., Tindle, A.G., 2007. A complex Petrogenesis for an Arc Magmatic Suite, St Kitts, Lesser Antilles. J. Petrol. 48, 3–42. https://doi.org/10.1093/petrology/egl052.
Traineau, H., Westercamp, D., Coulon, C., 1983. Mélanges magmatiques à la Montagne Pelée (Martinique) Origine des eruptions de type Saint - Vincent. Bull. Volcanol. 46, 243–269. https://doi.org/10.1007/BF02597560.

Underwood, S.J., Feeley, T.C., Clynne, M.A., 2012. Hydrogen isotope investigation of amphibole and biotite phenocrysts in silicic magmas erupted at Lassen volcanic center, California. J Volcanol Geotherm Res 227-228, 32–49.

Viccaro, M., Giacomoni, P.P., Ferlito, C., Cristofolini, R., 2010. Dynamics of magma supply at Mt. Etna volcano (Southern Italy) as revealed by textural and compositional features of plagioclase phenocrysts. Lithos 116, 77–91. https://doi.org/10.1016/j.lithos.2009.12.012.

Wadge, G., 1986. The dykes and structural setting of the volcanic from in the Lesser Antilles island arc. Bull. Volcanol. 48, 349–372.

Westercamp, D., Tazieff, H., 1980. Martinique, Guadeloupe, Saint-Martin. La Désirade, Masson, Paris, p. 135.

Westercamp, D., Traineau, H., 1983. The past 5,000 years of volcanic activity at Mt. Peléemartinique (F.W.I.): Implications for assessment of volcanic hazards. J. Volcanol. Geotherm. Res. 17, 159–185. https://doi.org/10.1016/0377 - 0273(83)90066 - 5.

Westercamp, D., Andreieff, P., Bouysse, P., Cottez, S., Battistini, R., 1989. Martinique; Carte géologique à 1/50000. In: BRGM, p. 246.

Zellmer, G.F., 2003. Geochemical Evolution of the Soufriere Hills Volcano, Montserrat, Lesser Antilles Volcanic Arc. J. Petrol. 44, 1349–1374. https://doi.org/10.1093/petrology/44.8.1349.

Ziberna, L., Green, E.C.R., Blundy, J.D., 2017. Multiple - reaction geobarometry for olivine - bearing igneous rocks. Am. Mineral. 102, 2349–2366. https://doi.org/10.2138/am - 2017 - 6154.